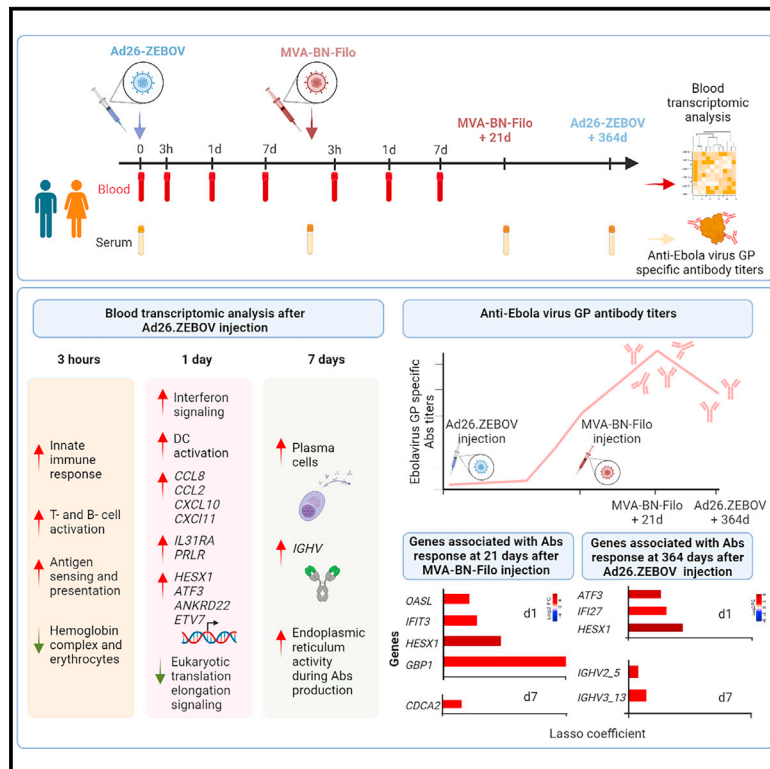


# Identification of early gene expression profiles associated with long-lasting antibody responses to the Ebola vaccine Ad26.ZEBOV/MVA-BN-Filo

## Graphical abstract



## Authors

Fabiola Blengio, Hakim Hocini, Laura Richert, ..., Kerstin Luhn, Rodolphe Thiebaut, Yves Levy

## Correspondence

rodolphe.thiebaut@u-bordeaux.fr (R.T.), yves.levy@aphp.fr (Y.L.)

## In brief

Blengio et al. investigate blood gene expression in volunteers receiving Ad26.ZEBOV/MVA-BN-Filo Ebola vaccines. Gene expression changes occurred 3 h post-prime. Specific genes of innate and adaptive immune responses are correlated with the magnitude and durability of antibody response 21 and 364 days after vaccinations.

## Highlights

- Ebola vaccination induces early gene modulation associated with durable antibody response
- HESX1, IFI27, and ATF3 upregulation at day 1 post-vaccination correlates with antibody levels
- IGHV3\_13 and IGHV2\_5 upregulation at day 7 post-vaccination correlates with antibody response



## Article

# Identification of early gene expression profiles associated with long-lasting antibody responses to the Ebola vaccine Ad26.ZEBOV/MVA-BN-Filo

Fabiola Blengio,<sup>1,6</sup> Hakim Hocini,<sup>1,6</sup> Laura Richert,<sup>1,2,3</sup> Cécile Lefebvre,<sup>1</sup> Mélyny Durand,<sup>2,3</sup> Boris Hejblum,<sup>1,2,3</sup> Pascaline Tisserand,<sup>1</sup> Chelsea McLean,<sup>4</sup> Kerstin Luhn,<sup>4</sup> Rodolphe Thiebaut,<sup>1,2,3,\*</sup> and Yves Levy<sup>1,5,7,\*</sup>

<sup>1</sup>Vaccine Research Institute, Université Paris-Est Créteil, Faculté de Médecine, INSERM U955, Team 16, Créteil, France

<sup>2</sup>University Bordeaux, Department of Public Health, INSERM Bordeaux Population Health Research Centre, Inria SISTM, UMR 1219, Bordeaux, France

<sup>3</sup>CHU de Bordeaux, Pôle de Santé Publique, Service d'Information Médicale, Bordeaux, France

<sup>4</sup>Janssen Vaccines & Prevention, B.V. Archimedesweg, Leiden, the Netherlands

<sup>5</sup>Assistance Publique-Hôpitaux de Paris, Groupe Henri-Mondor Albert-Chenevier, Service Immunologie Clinique, Créteil, France

<sup>6</sup>These authors contributed equally

<sup>7</sup>Lead contact

\*Correspondence: [rodolphe.thiebaut@u-bordeaux.fr](mailto:rodolphe.thiebaut@u-bordeaux.fr) (R.T.), [yves.levy@aphp.fr](mailto:yves.levy@aphp.fr) (Y.L.)

<https://doi.org/10.1016/j.celrep.2023.113101>

**SUMMARY**

Ebola virus disease is a severe hemorrhagic fever with a high fatality rate. We investigate transcriptome profiles at 3 h, 1 day, and 7 days after vaccination with Ad26.ZEBOV and MVA-BN-Filo. 3 h after Ad26.ZEBOV injection, we observe an increase in genes related to antigen presentation, sensing, and T and B cell receptors. The highest response occurs 1 day after Ad26.ZEBOV injection, with an increase of the gene expression of interferon-induced antiviral molecules, monocyte activation, and sensing receptors. This response is regulated by the HESX1, ATF3, ANKRD22, and ETV7 transcription factors. A plasma cell signature is observed on day 7 post-Ad26.ZEBOV vaccination, with an increase of *CD138*, *MZB1*, *CD38*, *CD79A*, and immunoglobulin genes. We have identified early expressed genes correlated with the magnitude of the antibody response 21 days after the MVA-BN-Filo and 364 days after Ad26.ZEBOV vaccinations. Our results provide early gene signatures that correlate with vaccine-induced Ebola virus glycoprotein-specific antibodies.

**INTRODUCTION**

Ebola virus disease (EVD) is an emerging zoonotic disease with intermittent outbreaks in Central and West African countries. EVD is characterized by a high fatality rate (varying between 50% and 90%)<sup>1</sup> and limited availability of specific therapies. Currently, two vaccines have been licensed, the Merck's Ervebo (rVSV-ZEBOV) and Johnson and Johnson two-dose combination of adenovirus-based Zabdeno vaccine (Ad26.ZEBOV) and the modified vaccinia Ankara-based Mvabea vaccine (MVA-BN-Filo). The recombinant rVSV-ZEBOV-GP vaccine showed high protection in a ring vaccination trial that immunized contacts and contacts of contacts of confirmed patients in Guinea.<sup>2,3</sup> rVSV-ZEBOV-GP elicits a strong and durable antibody response that correlates with the early activation of innate immunity, especially of monocytes and type I interferon-induced genes.<sup>4–6</sup>

Preclinical studies of the Zabdeno and Mvabea two-dose immunization showed full protection of nonhuman primates (NHPs) against an Ebola virus challenge.<sup>7</sup> Phase 1/2 studies in European and African adults, adolescents, and children showed acceptable safety and tolerability of the vaccine. The Zabdeno and Mvabea two-dose vaccine elicited a strong Ebola virus glycoprotein (GP)-specific immunoglobulin G (IgG) neutralizing anti-

body response, along with both CD4<sup>+</sup> and CD8<sup>+</sup> T cell responses.<sup>8–17</sup> Antibodies persisted beyond 1 year, and up to 3 years, after vaccination.<sup>10,18</sup> Among the complex immune response, the antibody response to Ebola virus GP is an important component of protection.<sup>9,19,20</sup> Hence, a sustained Ebola virus GP-specific antibody response to rVSV-ZEBOV vaccination was found to correlate with the early activation of innate immunity, monocytes, and type I interferon-induced genes.<sup>4–6</sup> Ad26.ZEBOV, followed by MVA-BN-Filo vaccination, induced the proliferation of less highly differentiated natural killer (NK) cells, accompanied by a robust and durable antibody-dependent NK cell response.<sup>21,22</sup>

Transcriptomic signatures have been used as markers of mechanisms involved in the innate and adaptive immune response induced by several vaccines such as those against yellow fever,<sup>23</sup> malaria,<sup>24</sup> influenza,<sup>25,26</sup> dengue,<sup>27</sup> and Ebola.<sup>28,29</sup> A gene expression signature that correlates with antibody titers has also been identified in response to the rVSVΔG-ZEBOV-GP vaccine.<sup>5,28,29</sup> In the present study, we extended these data with the analysis of the gene expression signature of the Ad26.ZEBOV and MVA-BN-Filo vaccine regimen. Here, we performed gene expression profiling to get an insight into the mechanisms involved in the innate and adaptive response after the Ad26.ZEBOV and





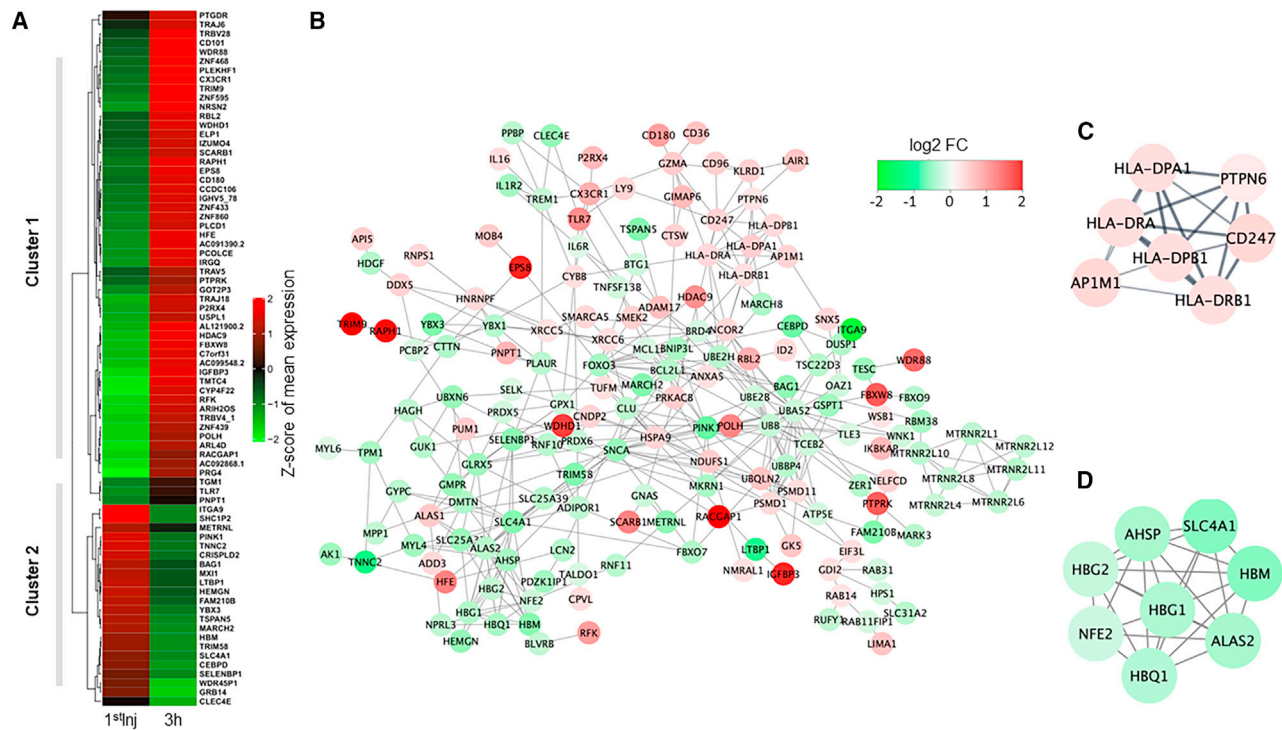


**Figure 2. Heatmap and main associated pathways of DEGs at 3 h after Ad26.ZEBOV injection**

(A) Heatmap of 76 DEGs with a  $\log_2$  FC  $\geq 0.58$  3 h after Ad26.ZEBOV administration relative to baseline.

(B) Gene regulatory network inference analysis of 230 DEGs with FDR  $\leq 0.05$ . Red and green indicate up- and downregulated genes, respectively.

(C and D) Main clusters identified by the Molecular Complex Detection (MCODE) analysis. The number of samples used in transcriptome analysis at baseline and 3 h after Ad26.ZEBOV administration were 50 and 49, respectively.

the two main clusters (Figure 2A). The first cluster corresponded to the upregulation of genes involved in the innate immune response, such as *TLR7*; *CX3CR1*<sup>32,33</sup>; *CD180*, a TLR-like protein mainly expressed on B cells, regulating proliferation and activation<sup>34</sup>; and *ZNF860*, a transcription factor (TF) that was recently reported to be associated with the B cell response.<sup>35</sup> Interestingly, at this early time point, many genes encoding the B and T cell repertoire were also upregulated, such as *TRAJ18*, *TRAJ6*, *TRAV5*, *TRBV28*, *TRBV4-1*, and *IGHV5-78*, suggesting rapid stimulation of T and B cells. The second main cluster was associated with the hemoglobin complex and erythrocyte development, such as *HBM*, *HEMGN*, and *PINK1*,<sup>36–38</sup> highlighting the role of erythrocytes in immune regulation.<sup>39–41</sup> We next performed a protein-protein interaction (PPI) network analysis to identify the main networks associated with the DEGs 3 h post-Ad26.ZEBOV injection using all 260 genes with an FDR  $\leq 0.05$  (Figure 2B), regardless of fold change. Our results highlight two main clusters that were consistent with the changes in gene expression described above. The first network is associated with T cell activation, with the upregulation of key genes of the T cell response, such as *CD247* (T cell surface GP CD3 zeta chain) and *PTPN6* (protein tyrosine phosphatase non-receptor type 2), and those of antigen-presenting cells, such as *HLA-DRB1*, *HLA-DPB1*, *HLA-DRA*, and *HLADPA1* (Figure 2C). The second network (Figure 2D) included downregulated genes of erythrocytes (*HBG1*, *HBM*, *HBG2*, *HBQ1*, *AHSP*, *SLC4A1*, and *ALAS2*).

### Ad26.ZEBOV induces innate immune and stress responses within 1 day post-administration

Next, we examined the transcriptomic changes at day 1 post-injection of Ad26.ZEBOV. Among the 2413 DEGs with a  $\log_2$  FC  $\geq 0.58$  relative to baseline, 795 were upregulated and 1,618 were downregulated. The results of the pathway analysis using Ingenuity Pathway Analysis software and based on the significance of the enrichment (corrected p value) with the predicted activated or inhibited function (positive and negative Z scores, respectively) are shown in Figure 3A. Globally, the main inhibited pathways corresponded to stress and protein translation, including eukaryotic initiation factor 2 (EIF2), mTOR, and the regulation of eIF4 and p70S6K signaling. Viruses require host-cell components to replicate and can utilize the cell's translational machinery, including eIF4F.<sup>42</sup> In contrast, pathways related to innate immune activation, including interferon (IFN) signaling, pattern recognition receptors, TREM1 signaling, the inflammasome, and dendritic cell maturation were predicted to be activated. Similarly, we also observed the upregulation of eukaryotic translation initiation F2 alpha kinase 2 (EIF2AK2), which encodes protein kinase R (PKR), a pattern recognition receptor that mediates antiviral responses.<sup>43</sup> Globally, these changes reflect features of Ad26 vaccine vector responses, which were confirmed by PPI analysis (Figure 3B). We identified three significant sub-networks selected from the 434 genes, of which the functions were mainly associated with eukaryotic translation elongation

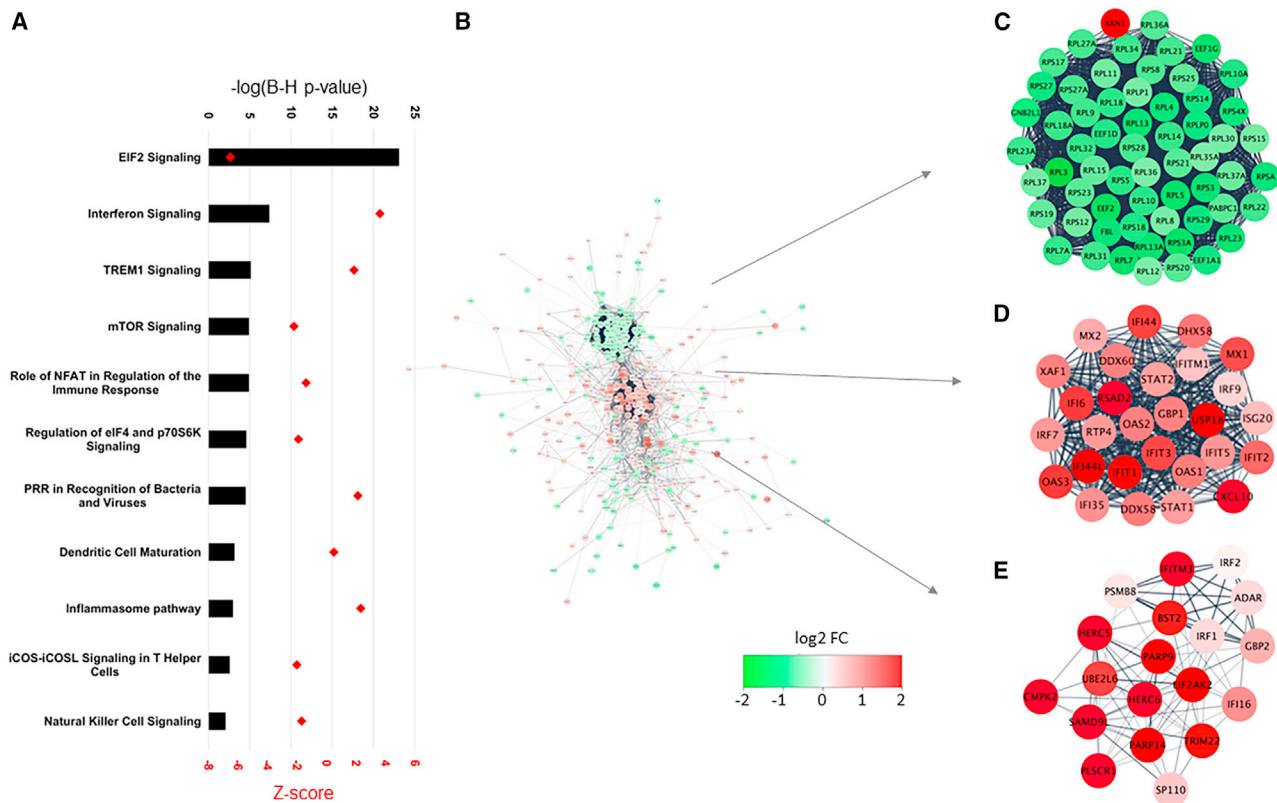


**Figure 3. Pathways associated with DEGs on day 1 after Ad26.ZEBOV injection**

(A) Top canonical pathways associated with 2413 DEGs with a  $\log_2 \text{FC} \geq 0.58$  observed at day 1 after Ad26.ZEBOV injection relative to baseline as determined using Ingenuity Pathway Analysis software. The Z score predicts the activation (Z score  $\geq 2$ ) or inhibition (Z score  $\leq -2$ ) of pathways.

(B) Gene regulatory network inference analysis of 2,413 genes. Red and green indicate up- and downregulated genes, respectively.

(C–E) Main clusters identified by the MCODE analysis. Up- and downregulated genes are represented in red and green, respectively. The number of samples used in transcriptome analysis at baseline and day 1 after Ad26.ZEBOV administration were 50 and 47, respectively.

(Figure 3C) and IFN signaling (Figures 3D and 3E). Of note, we observed strong upregulation of the *XRN1* gene (5'-3' exoribonuclease 1), known for its role as a decay factor, which was recently shown to be associated with antiviral activity against RNA viruses.<sup>44</sup> In parallel, Ad26.ZEBOV induced the upregulation of genes induced by IFNs, such as TFs (*IRF9*, *IFI6*, *IFIT5*, and *IFIT1*); nucleic acid sensors (*DDX58* and *DHX58*); oligoadenylate synthases (*OAS3* [2'-5'-oligoadenylate synthetase 3] and *OAS2*), which are double-stranded (ds) RNA-activated enzymes; an antiviral enzyme (*RSAD2* [radical S-adenosyl methionine domain-containing 2]); and an IFN-stimulated gene (*USP18*) (Figure 3D). Finally, we noted the upregulation of *EIF2AK2*, *HERC5* [HECT and RLD domain-containing E3 ubiquitin protein ligase 5], and *HERC6*, which mediates ISGylation in response to IFN stimulation,<sup>45</sup> and *IFITM3*, which belongs to the family of IFN-induced antiviral proteins (Figure 3E). The prediction of cell populations through the deconvolution of DEGs at day 1 showed significant enrichment of memory T and B cells, M1 and M2 macrophages, and activated dendritic cells (DCs). By contrast, naive B cells and M0 macrophages were less abundant (Figure S1). Next, we sought to analyze the main longitudinal changes in gene expression at various time points following heterologous vaccination. We observed major changes in gene expression

at day 1 after each vaccination, with the highest number of DEGs following Ad26.ZEBOV injection. Two contrasting profiles of genes encoding the cytokine response were observed on day 1 (Figure 4A). The first profile consisted of downregulated proinflammatory genes: *IL-32*, *CCL5*, *CXCL8*, *IL23A*, *CXCL6*, *CXCL1*, and *CCL28*.<sup>46</sup> The second profile included upregulated genes encoding IFN-stimulated genes (*CXCL9*, *CXCL11*, and *CXCL10*) and monocyte and lymphocyte chemoattractants, such as *CCL1* (monocyte chemoattractant protein 1), *CCL2*, *CCL8*, and *CCL7*. The expression of cytokine genes was highest at day 1 post-first injection relative to other time points (Figure 4B).

As cytokines trigger the immune response through binding to membrane receptors expressed on immune cells, we also looked for changes in receptor gene expression on day 1 (Figure 4C). The most highly upregulated receptor was interleukin-31 receptor A (IL-31RA), the receptor of IL-31, a cytokine primarily secreted by activated helper T cells.<sup>47,48</sup> IL-31RA is mainly expressed by immune cells, such as activated monocytes, macrophages, and DCs.<sup>47,48</sup> In addition, many members of the Fc $\gamma$ R family genes (*FCER1A*, *FCER1G*, *FCGR1B*, *FCGR2B*, *FCGR2C*, *FCGR3A*, and *FCGR3B*) were also upregulated, showing the strong involvement of myeloid cells, probably

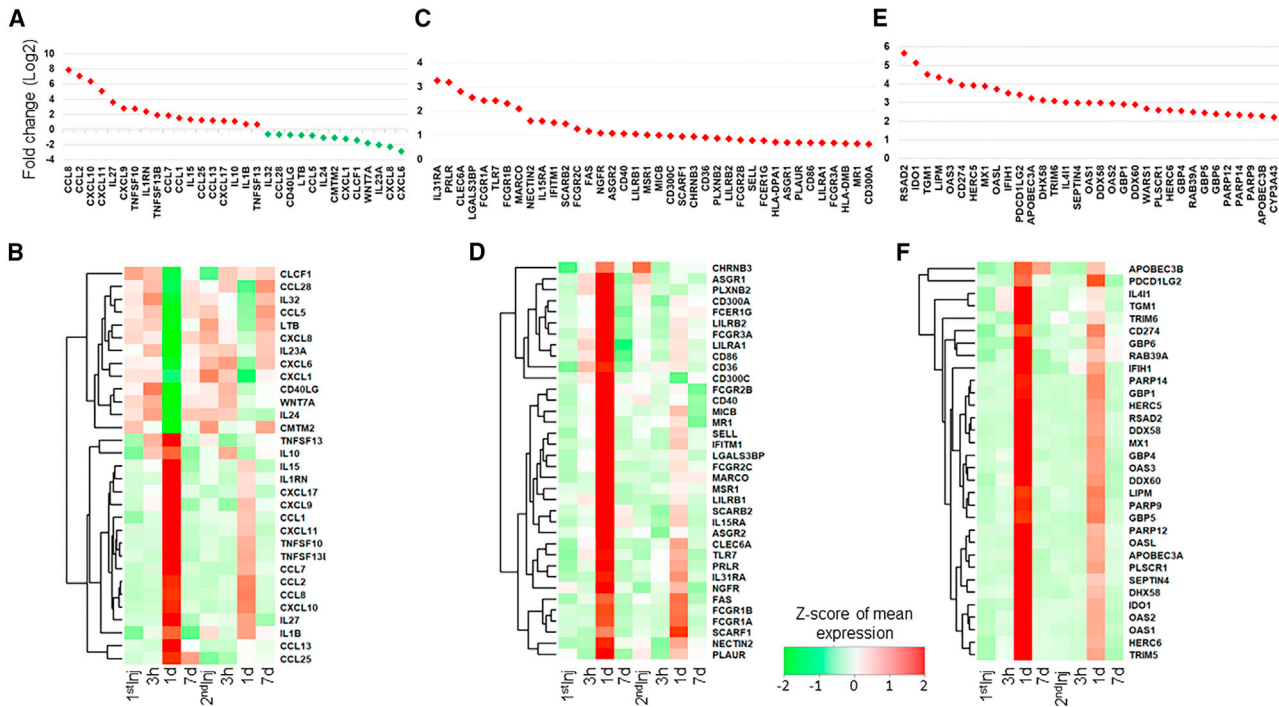


**Figure 4. DEGs of encoded cytokines, receptors, and enzymes on day1 after Ad26.ZEBOV injection**

(A) Top genes encoding cytokines at day 1 after Ad26.ZEBOV injection.  
 (B) Heatmap of the kinetics of expression of top DEGs encoding cytokines at day 1 after Ad26.ZEBOV injection relative to baseline. Ad26.ZEBOV injection (1<sup>st</sup>Inj). MVA-BN-Filo injection (2<sup>nd</sup>Inj).  
 (C) Top upregulated genes encoding receptors on day 1 after Ad26.ZEBOV injection.  
 (D) Heatmap of the kinetics of expression of top DEGs encoding receptors at day 1 after Ad26.ZEBOV injection relative to baseline. Ad26.ZEBOV injection (1<sup>st</sup>Inj). MVA-BN-Filo injection (2<sup>nd</sup>Inj).  
 (E) Top upregulated genes encoding enzymes on day 1 after Ad26.ZEBOV injection.  
 (F) Heatmap of the kinetics of expression of top DEGs encoding receptors at day 1 after Ad26.ZEBOV injection relative to baseline. Ad26.ZEBOV injection (1<sup>st</sup>Inj). MVA-BN-Filo injection (2<sup>nd</sup>Inj). Up- and downregulated genes are indicated in red and green, respectively. The number of samples used in transcriptome analysis at baseline and day 1 after Ad26.ZEBOV administration were 50 and 47, respectively.

triggered by immune complexes generated during the immunization.<sup>49</sup> Furthermore, many genes encoding pathogen-recognition receptors were overrepresented, such as macrophage and DC receptors with collagenous structure (*MARCO*), macrophage scavenger receptor 1 (*MSR1*), *CD36*, and Toll-like receptor 7 (*TLR7*), an endosomal sensor that recognizes viral single-stranded RNA (ssRNA), expressed mainly on plasmacytoid DCs.<sup>50,51</sup> Interestingly, *MARCO* is associated with adenovirus infection in mice and efficient innate virus recognition through the cytoplasmic DNA sensor *cGAS*, leading to strong proinflammatory responses.<sup>52</sup> Of note, a number of these genes were highly upregulated on day one after the first and second injections, such as *IL31RA*, *PRLR*, *IFITM1*, *IL15RA*, *FCGR1A*, *FCGR1B*, *TLR7*, *MICB*, *SCARB2*, *CLEC6A*, *NGFR*, *FAS*, and *SCARF1*, expressed on presenting DCs.<sup>53</sup> The expression of receptor genes was highest on day 1 post-first injection and did not reach the same level on day 1 after the second injection (Figure 4D).

On the other hand, as immunometabolism has an important role in the establishment and regulation of the innate and adaptive immune response, we looked for the most highly upregulated genes encoding enzymes (Figure 4E). We observed a

higher response on day 1 after injection with the Ad26.ZEBOV than with the MVA-BN-Filo vaccine (Figure 4F), with the upregulation of antiviral genes, such as *RSAD2*<sup>54</sup>, *OAS3*, which inhibits viral replication through the activation of RNaseL<sup>55</sup>, and *HERC5*, which has a fundamental role in ISGylation viral proteins, leading to the inhibition of viral replication.<sup>56</sup> In parallel, we observed the upregulation of regulatory genes, such as *IDO1* (indoleamine 2,3-dioxygenase 1), an IFN type I (IFN-I)- and IFN-II-induced enzyme,<sup>57</sup> that is a checkpoint controller with a suppressive function on innate and adaptive immunity through catabolism of the amino acid tryptophan; *TGM1* (transglutaminase 1), which activates molecular signatures of antimicrobial and innate defense responses in skin when downregulated<sup>58</sup>; and *CD274*, a gene that encodes an immune inhibitory receptor that inhibits T cell activation and cytokine production, preventing a deleterious immune response.<sup>59</sup> Globally, these analyses highlight the finely tuned balance between the regulation of viral vector replication and the avoidance of an immune over-response to the vaccine.

Next, we identified changes in gene expression of key TFs that regulate the early steps of the immune response from day 1 after Ad26.ZEBOV injection (Figure 5A). In particular, the analyses

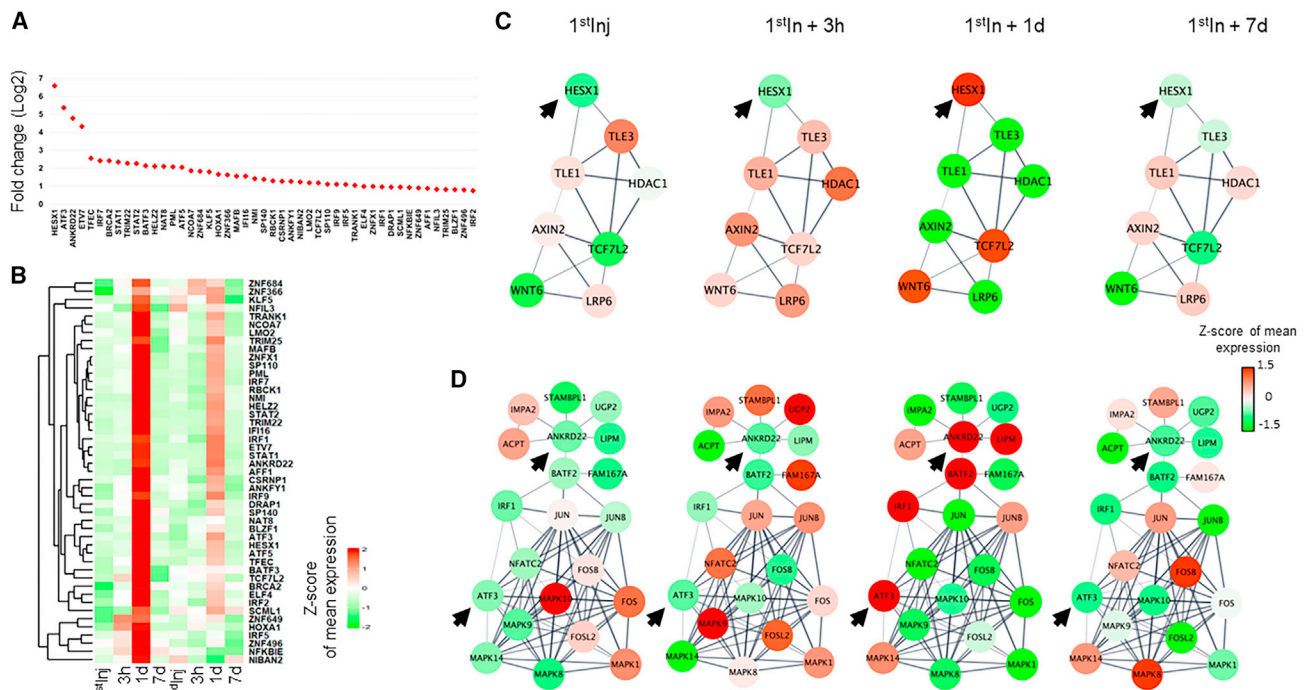


**Figure 5. Top upregulated DEGs encoding transcription factors on day 1 after Ad26.ZEBOV injection**

(A) Top upregulated DEGs encoding TFs on day 1 after Ad26.ZEBOV injection.

(B) Heatmap of the kinetics of expression of top DEGs encoding TFs at day 1 after Ad26.ZEBOV injection relative to baseline. Ad26.ZEBOV injection ( $1^{st}Inj$ ). MVA-BN-Filo injection ( $2^{nd}Inj$ ).

(C and D) PPI network of HESX1 (C) and of ANKRD22 (D) TFs. PPIs were analyzed using STRING software, showing the kinetics of gene expression at baseline, 3 h, and 1 and 7 days after Ad26.ZEBOV injection. Up- and downregulated genes are indicated in red and green, respectively. The number of samples used in transcriptome analysis at baseline and day 1 after Ad26.ZEBOV administration were 50 and 47, respectively.

revealed the overexpression of four main TFs, including HESX homeobox 1 (*HESX1*), a homeobox transcriptional repressor,<sup>60</sup> expressed in activated monocyte-derived DCs<sup>61</sup>; activating TF3 (*ATF3*), which can modulate the expression of a variety of genes to limit excessive inflammation<sup>62</sup>; ankyrin repeat domain 22 (*ANKRD22*), which mediates the host defense against viral infection through the STING signaling pathway<sup>63</sup>; and ETS variant TF 7 (*ETV7*), an IFN-stimulated gene involved in hematopoiesis and antiviral responses.<sup>64</sup> The upregulation of TFs was stronger on day 1 after Ad26.ZEBOV than after MVA-BN-Filo vaccination (Figure 5B). To obtain further insight into the molecular mechanisms of TF activity at each time point (baseline, 3 h, 1 day, and 7 days after Ad26.ZEBOV injection), we first generated a PPI network for the HESX1 and ATF3-ANKRD22 TF axis (Figures 5C and 5D). The highest observed expression of *HESX1* was on day 1 and corresponded with lower expression of *TLE3*, *TLE1*, *HDAC1*, *AXIN2*, and *LRP6* and with higher expression of *TCF7L2* and *WNT6* (Figure 5C). This pattern was inverted at 3 h, with *HESX1* expression lower than that of the other genes. Interestingly, on day 7, this pathway profile had returned to baseline expression (Figure 5C). The second important TFs engaged at day 1 post-vaccination consisted of the ANKRD22-BATF2-IRF1-ATF3-MAPK3 network axis (Figure 5D), which also interacts with FOS and JUN, members of AP-1 transcriptional complexes.<sup>9</sup> Similarly, ATF3 plays a key role in regulating immune responses

and maintaining normal host defenses.<sup>65</sup> We have also identified ETV7 as an important TF engaged at day 1 post-vaccination. PPI analysis showed that ETV7 is connected to ETV6 and KLF11, which are also overexpressed at day 1 after Ad26.ZEBOV injection (Figure S2). ETV7 and ETV6 have been demonstrated to play key roles in hematopoiesis, particularly in maintenance of hematopoietic stem cells and control of lineage-specific differentiation.<sup>66</sup> Recently, ETV7 was reported as playing an important role as a negative regulator of the IFN-I response.<sup>64</sup> Interestingly, albeit of lower magnitude, a similar profile of transcriptomic changes was also observed on day 1 post-MVA-BN-Filo injection, highlighting day 1 as a key endpoint for the analysis of transcriptomic changes associated with the response to vaccination. Aside from these TFs, many others were also upregulated, mainly IFN-induced factors, such as *IFI16*, *IRF1*, *IRF5*, *IRF7*, and *IRF9*, as well as the zinc-finger proteins *ZNF366*, *ZNF496*, *ZNF649*, *ZNF684*, and *ZNFX1*, which are involved in the regulation of multiple steps of RNA metabolism and the immune response by targeting mRNA for degradation and thus modulation signaling pathways.<sup>67</sup>

#### Ad26.ZEBOV induces changes in B cell gene expression within 7 days after administration

On day 7 post-Ad26.ZEBOV injection, we found 460 DEGs with a  $\log_2$  FC  $\geq 0.58$  relative to baseline (25 downregulated and 435

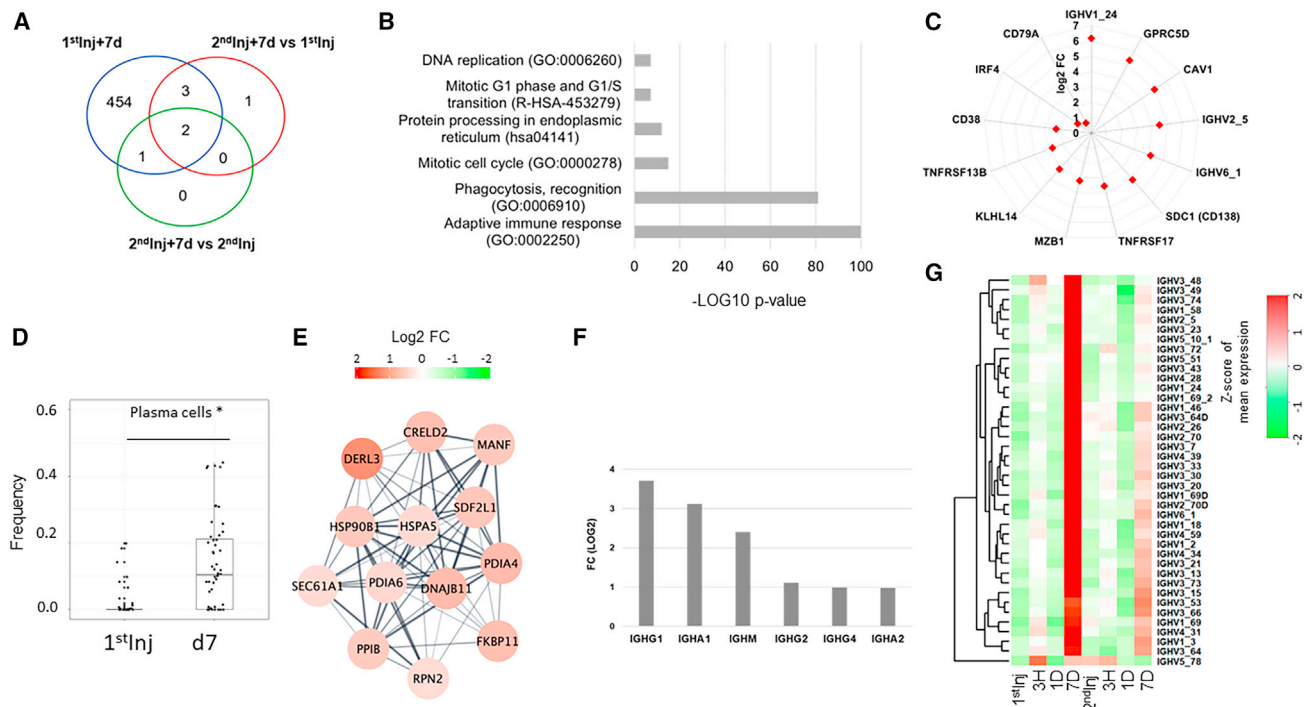


**Figure 6. DEGs at 7 days after Ad26.ZEBOV vaccination**

- (A) Venn diagram showing the number of DEGs on day 7.  
 (B) Pathways associated with 460 DEGs with a log<sub>2</sub> FC ≥ 0.58 as analyzed by Metascape software.  
 (C) Main plasma B cell markers of DEGs on day 7.  
 (D) Cell deconvolution analysis of 460 DEGs on day 7 after Ad26.ZEBOV administration. The cell composition was inferred using the CIBERSORT algorithm implemented in the tidybulk package in R Bioconductor. The medians of the frequencies of immune cells are shown in the boxplots. The boxes represent the interquartile range (IQR), and the whiskers represent the largest and smallest values. Only cell populations that showed a significant difference between groups (\*Welch t test  $p \leq 0.05$ ) are displayed.  
 (E) Weighted coexpression network obtained from the MCODE of DEGs on day 7 that allow visualization of the significant gene modules in the network. Up- and downregulated genes are depicted in red and green, respectively.  
 (F) Immunoglobulin isotype DEGs on day 7 after Ad26.ZEBOV administration.  
 (G) Heatmap of the kinetics of expression of DEGs at day 7 encoding IGHV chains. Ad26.ZEBOV injection (1<sup>st</sup>Inj). MVA-BN-Filo injection (2<sup>nd</sup>Inj). The number of samples used in transcriptome analysis at baseline and day 7 after Ad26.ZEBOV administration were 50 and 44, respectively.

upregulated), whereas very few DEGs were found on day 7 after MVA-BN-Filo injection relative to either the baseline of the Ad26.ZEBOV or the MVA-BN-Filo injection (Figure 6A). Pathway enrichment analysis showed the B cell adaptive immune response to be the most predominant, followed by phagocytosis and mitotic cell division (Figure 6B). Among the upregulated DEGs (Figure 6C), many encode proteins associated with B and plasma cells, such as TNFRSF13B, which has a crucial role in humoral immunity by interacting with two members of the TNF family, BAFF and APRIL, and by driving the differentiation of B cells into long-lived plasma cells,<sup>68</sup> TNFRSF17, which is expressed in mature B lymphocytes and encodes the ligand of TNFRSF13, marginal zone B and B1 cell specific protein (MZB1),<sup>69</sup> and CD79A, a B cell antigen receptor complex, as well as CD38, a cell activation marker.<sup>70</sup> Interestingly, we observed increased expression of the novel tumor-suppressor *KLHL14* (Kelch-like family member 14) gene, of which the protein promotes the ubiquitylation of B cell receptor (BCR) subunits and decreases the stability of immature BCR forms in the endo-

plasmic reticulum, thus reducing BCR levels associated with plasma cell differentiation. This mechanism is crucial for controlling the central functions of the BCR during the development and activation of normal B cell subpopulations during the immune response to vaccines.<sup>71</sup> This was supported by deconvolution analysis,<sup>72</sup> confirming the increase in the plasma cell population (t test  $\leq 0.05$ ) at day 7 post-Ad26.ZEBOV injection (Figure 6D). Subsequently, we performed PPI analysis of the 460 DEGs. The most significant cluster to emerge from Molecular Complex Detection (MCODE) analysis (Figure 6E) was enriched for genes encoding proteins that are central orchestrators of the molecular mechanism of endoplasmic reticulum activity during Ig production, such as PDIA4 and PDIA6,<sup>73</sup> HSPA5, and HSP90B1, heat shock proteins that play an important role in B cell function by maintaining protein homeostasis in the endoplasmic reticulum and binding to Igs.<sup>74</sup> Overall, these findings indicate that, on day 7, the Ad26.ZEBOV response includes the endoplasmic reticulum (ER) machinery to allow the production and secretion of copious amounts of Igs.<sup>75</sup> This was confirmed by the enrichment



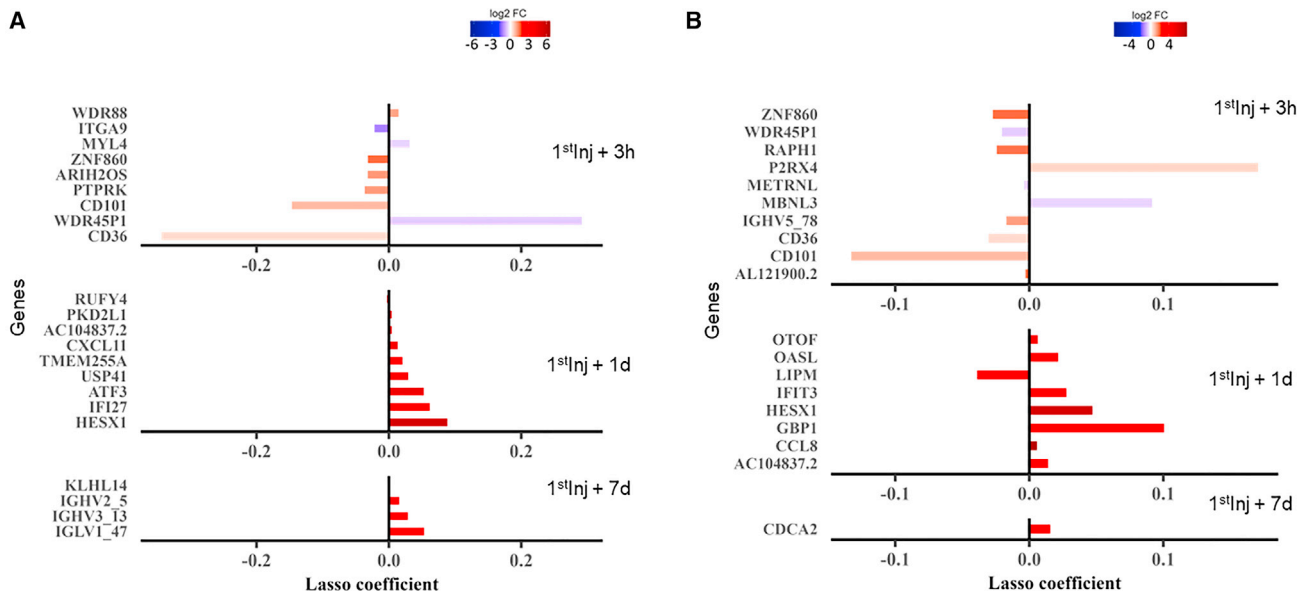


**Figure 7. Genes correlating with the magnitude of antibody response at 364 days post-Ad26.ZEBOV and 21 days post-MVA-BN-Filo vaccinations**

(A) DEGs at 3 h, day 1, and day 7 that correlate with the magnitude of antibody response at 364 days after Ad26.ZEBOV injection.

(B) DEGs at 3 h, day 1, and day 7 that correlate with the magnitude of antibody response at 21 days after MVA-BN-Filo injection. The downregulated and up-regulated DEGs were expressed in log<sub>2</sub> FC as compared with before vaccination and are displayed in blue and red, respectively. Lasso analysis was performed using the 100 most modulated DEGs (FDR-adjusted  $p \leq 0.05$ , ranked by FC) at a given time point as potential correlates. The Lasso coefficient (shown on the x axis) is interpreted like a regression coefficient.

of genes coding for the B cell repertoire, as 193 Ig genes were upregulated. The antibody response to Ad26.ZEBOV was represented by IGHG1, IGHA1, IGHM, IGHG2, IGHG4, and IGHA2 isotypes (Figure 6F). The response of the IGHV genes over time highlights the fact that certain IGHV genes were strongly upregulated at day 7 after the injection of Ad26.ZEBOV, as well as of MVA-BN-Filo (Figure 6G), whereas others were less highly expressed at day 7 after MVA-BN-Filo injection. Interestingly, within the bimodal IGHV response, we observed *IGHV3\_13* and *IGHV3\_15*, which were already shown as associated with Ebola virus GP neutralizing antibody response,<sup>9,76,77</sup> as well as novel IGHV genes, such as *IGHV2\_5*, *IGHV6\_1*, and *IGHV2\_70*. On the contrary, *IGHV3\_48*, *IGHV5\_51*, *IGHV1\_24*, and *IGHV1\_69\_2* did not peak 7 days after MVA-BN-Filo injection. Of note, *IGHV3\_48* was also induced 3 h after the first injection.

#### DEGs at 3 h and 1 and 7 days after Ad26.ZEBOV administration were associated with antibody response levels

The Ad26.ZEBOV and MVA-BN-Filo regimen induced a robust antibody response, as demonstrated in the EBL2001 clinical trial<sup>16</sup> where the total IgG Ebola virus GP-specific binding antibody concentrations were measured by the use of an Ebola virus GP Filovirus Animal Non-Clinical Group ELISA at Q2 Solutions Laboratories (San Juan Capistrano, CA, USA).<sup>16,78,79</sup> The kinetics of the specific IgG binding antibody response to the GP of the Ebola Zaire virus (Mayinga variant) started at a median of 18 (interquartile range: 18–18) ELISA units/mL before injection of Ad26.ZEBOV, increased to 599 (350–1,240) ELISA

units/mL on the day of the MVA-BN-Filo injection, peaked at 8,185 (4,745–11,708) ELISA units/mL 21 days following the MVA-BN-Filo boost, and persisted at 1,033 (647–2,087) ELISA units/mL on day 364. We observed a similar antibody response profile when the data were expressed as the geometric mean with accompanying 95% confidence interval (Table S1). The vaccine-induced antibody response exhibited a strong neutralization ability as measured by pseudovirion neutralization assay at Monogram (San Francisco, CA, USA).<sup>16</sup> Furthermore, there were strong correlations between GP-binding antibody concentrations and neutralizing antibody titers measured after completion of the two-dose vaccination regimen.<sup>16</sup> We applied a Lasso approach<sup>80</sup> to identify changes in gene expression at 3 h, 1 day, and 7 days after Ad26.ZEBOV injection associated with the total IgG Ebola virus GP-specific response. We identified genes that correlated with the antibody response 1 year after the Ad26.ZEBOV vaccine injection (Figure 7A). Indeed, at 3 h, the downregulated WD repeat domain 45 pseudogene 1 (*WDR45P1*) was positively correlated with the antibody response at 364 days after Ad26.ZEBOV injection. In contrast, the upregulated *CD36* and *CD101* genes were negatively correlated with this antibody response. At day 1, we identified *HESX1*, IFN alpha inducible protein 27 (*IFI27*), and *ATF3*<sup>81</sup> as the genes that positively correlated with the antibody response at 1 year after the first vaccination. At day 7, the best-correlating genes with the response at 1 year were associated with the plasma cell response and consisted of the Ig heavy and light variable genes *IGHV3\_13*, *IGHV2\_5*, and *IGLV1\_47*.

Furthermore, we also identified the *CD101* followed by *CD36*, Ras association (RalGDS/AF-6) and pleckstrin homology domains 1 (*RAPH1*), zinc-finger protein 860 (*ZNF860*), and *IGHV5\_78* genes at 3 h after Ad26.ZEBOV injection as the top negative correlates with the magnitude of the GP-specific antibody response at 21 days after MVA-BN-Filo injection (Figure 7B). Inversely, the purinergic receptor P2X4 (*P2RX4*) and muscle blind-like splicing regulator 3 (*MBNL3*) were the best positive correlates with the magnitude of the antibody response at 21 days after MVA-BN-Filo injection. Similarly, the expression at day 1 of guanylate-binding protein 1 (*GBP1*), *HESX1*, IFN-induced protein with tetratricopeptide repeats 3 (*IFIT3*), and *OAS*-like (*OASL*) positively correlated with the antibody response at 21 days after MVA-BN-Filo injection. On day 7, the most positively correlated gene expression was the cell division cycle-associated 2 (*CDC42*) gene.

## DISCUSSION

We aimed to identify gene signatures following a heterologous two-dose regimen with the Ad26.ZEBOV and MVA-BN-Filo vaccines in healthy volunteers enrolled in the randomized phase 2 EBL 2001 EBOVAC study (<https://clinicaltrials.gov/ct2/show/NCT02416453>). The results highlight the main early mechanisms that govern the establishment of efficient innate and adaptive immune responses to Ebola virus GP. Globally, the transcriptional responses to both vaccines peaked at day 1 post-injection, with a stronger transcriptional response after the Ad26.ZEBOV than MVA-BN-Filo injections. We observed significant changes in expression of genes relative to the status before vaccination within as little as 3 h after Ad26.ZEBOV injection, which reached its maximum on day 1 and included genes encoding molecules associated with the innate immune response, preceding a strong plasma cell signature on day 7. These observations are in agreement with the results of comparative analysis of immunity to 13 vaccines, showing that most vaccines induce innate immunity and plasmablast signatures at days 1 and 7 after vaccination, respectively.<sup>82</sup> We also identified gene expression signatures at 3 h and 1 and 7 days after Ad26.ZEBOV injection, which correlated with the magnitude of the vaccine antibody response to Ebola virus GP up to 1 year from the baseline. Our study demonstrates that early events post-vaccine injection are critical to provide insights into the molecular mechanism that may be associated with robust and protective immunity. 3 h after Ad26.ZEBOV injection, we observed changes in genes involved in erythropoiesis, which could indicate a role for these cells in vaccine responses since red blood cells can regulate inflammation by binding cytokines and chemokines or by regulating immune cells directly.<sup>83,84</sup> We also observed increased expression of many alpha and beta TCR clone genes (*TRAJ18*, *TRAJ6*, *TRAV5*, *TRBV28*, *TRBV4-1*), supporting the hypothesis of either the activation of pre-existent adenovirus-specific memory T cell subsets<sup>85,86</sup> or of cross-reactive T cells to other vaccines, such as influenza.<sup>87</sup> This observation is consistent with the observed increased B cell gene expression, also suggesting an expansion of cross-reactive memory B cell responses to adenoviruses. This hypothesis was supported by the upregulation of two genes, *CD180* and *ZNF860*, reported to be potent factors involved in

B cell activation and antibody maturation,<sup>35,88,89</sup> and increased levels of *IGHV3\_48* and *IGHV3\_39* transcripts, which were previously reported to belong to the adeno-associated virus (AAV) memory B cell IgG gene repertoire,<sup>90</sup> showing the potential involvement of adenoviral cross-reacting memory B cells within 3 h in the response to the Ad26.ZEBOV vaccine. This set of events associated with the early responses to Ad26.ZEBOV led to a substantial transcriptional change at day 1. Some of these changes, such as the activation of IFN signaling, were not specific to the Ad26.ZEBOV and MVA-BN-Filo vaccine regimen and are consistent with the response observed with Merck's Ervebo (rVSV-ZEBOV)<sup>28,29,91</sup> vaccine and with yellow fever,<sup>92</sup> HIV,<sup>93</sup> influenza,<sup>25</sup> and malaria<sup>24</sup> vaccines. Thus, our results are consistent with a recent work that compared the signatures of several vaccines and showed that there is a substantial set of common signatures, demonstrating the use of similar immunological pathways by various vaccines with different composition and antigens.<sup>82</sup> Here, we extended these data, highlighting a fine balance between these responses and waning of the inflammatory response, as illustrated by the inhibition of transcription of granulocyte-related cytokines, such as CXCL6, CXCL8, and CXCL1, and the upregulation of IL-31RA, of which the ligand is IL-31, a cytokine secreted by activated T cells, especially T helper (Th)2 cells.<sup>47,48</sup> Interestingly, this response was accompanied by the transcriptional inhibition of translation initiation genes, which could be the consequence of the upregulation of IFN-stimulated genes (ISGs), such as 2'-5'-oligoadenylate synthetase, which leads to perturbation of the translational machinery as an antiviral mechanism to limit host and viral mRNA translation.<sup>94,95</sup> In accordance with these observations, the upregulation of *eIF2AK2* observed at day 1 was associated with the downregulation of several ribosomal protein-encoding genes and, consequently, the inhibition of transcription of genes involved in mTOR and eIF4/p70S6K signaling. These data underline the prominence of the mTOR, EIF2, and eIF4/p70S6K axis in the establishment and regulation of the innate immune response to vaccines.

To better understand the regulatory mechanisms involved in the establishment of the immune response to Ad26.ZEBOV, it was essential to monitor the modulation of the expression of TFs at early time points. On day 1 post-Ad26.ZEBOV injection, we observed increased expression of several TFs regulating the IFN-induced genes as well as an overexpression of the four TFs, *HESX1*, *ATF3*, *ANKRD22*, and *ETV7*. Consistent with this finding, upregulation of *HESX1* was previously observed at day 1 post-rVSV-ZEBOV injection<sup>5</sup> and following malaria vaccination.<sup>24</sup> In our data, the upregulation of *HESX1* at day 1 was associated with switching off the Wnt signaling cascade (*LE3*, *TLE1*, *HDAC1*, *TCF7L2*, *AXIN2*, *LRP6*, and *WNT6*), which is a determinant of the fate of immune cell populations. The second important TFs engaged on day 1 consisted of *ANKRD22* and *ATF3*, which also interact with *FOS* and *JUN*, members of the AP-1 transcriptional complexes involved in a variety of cellular processes, regulation of the immune system,<sup>9,96,97</sup> and responses to DNA and RNA viruses.<sup>63</sup>

Aside from the innate response, the adaptive immune response signature was observed on day 7 after Ad26.ZEBOV vaccination, as shown by the upregulation of many plasma cell

markers, as well as that of genes encoding IG heavy chains.<sup>70</sup> This was confirmed by CIBERSORT, showing enrichment of the plasma cell population, consistent with the enrichment of transcripts of the IGHV gene family over time and the expansion of polyclonal B cell responses on day 7 post-Ad26.ZEBOV administration. Such a high level of expression precluded the observation of significant secondary enrichment post-MVA-BN-Filo injection. Interestingly, included in the bimodal IGHV response, we noted the presence of IGHV3\_13 and IGHV3\_15, which are reported to be associated with specific response to Ebola virus antigens,<sup>76</sup> as well as novel transcripts in the Ebola virus IGHV response, such as IGHV2\_5, IGHV6\_1, and IGHV2\_70. The plasma cell signature was not restricted to conventional plasma cell markers and IGH genes but also included enrichment of transcripts for genes involved in the ER machinery that drive the production and secretion of IGHs, as shown by the PPI analysis of DEGs on day 7 after Ad26.ZEBOV injection.<sup>98</sup> Furthermore, we observed increased expression of the novel tumor-suppressor *KLHL14*, which promotes the ubiquitylation of BCR subunits and decreases the stability of immature BCR forms in the endoplasmic reticulum, thus reducing BCR levels. This mechanism is crucial for controlling the functions of the BCR in the development and activation of normal B cell subpopulations during the immune response to vaccines.<sup>71</sup> In addition, the upregulation of genes essential for B cell development, such as *TNFRSF17* and *TNFRSF13B*,<sup>69</sup> which interact with two members of the TNF family, BAFF and APRIL, to drive the differentiation of B cells into long-lived plasma cells,<sup>68</sup> confirms the capacity of Ad26.ZEBOV injection to elicit a long-lasting antibody response. One unique aspect of this study was the identification of changes in gene expression at early time points after the Ad26-ZEBOV injection that correlated with the magnitude of vaccine-elicited antibody responses at day 21 post-MVA-BN-Filo and at 1 year post-Ad26.ZEBOV. For this, we carried out a Lasso approach. We identified the *CD101* and *CD36* genes at 3 h as being negatively correlated, and *P2RX4* and *MBNL3* as being positively correlated, with the magnitude of the antibody response at 21 days after MVA-BN-Filo injection. Similarly, *GBP1*, *HESX1*, and *IFIT3* gene expressions at day 1 were positively correlated with the magnitude of the antibody response at 21 days after MVA-BN-Filo injection. On day 7, the most highly correlated gene was *CDCA2*, a member of cell-cycle-related proteins that was associated with upregulation of immune checkpoints and regulation of immune response.<sup>99</sup> Although more challenging, we were able to identify the genes associated with the antibody response 364 days after Ad26.ZEBOV administration.

We showed that increases in *CD36* and *CD101* gene abundance were also correlated with response at day 364. Similarly, on day 1, we identified several correlates, including *HESX1*, *IFI27*, and *ATF3* as the three best positive correlates of the antibody response at 1 year after the first vaccination. Of note, *HESX1* was associated with the antibody magnitude both at 21 days post-MVA-BN-Filo and at 364 days after Ad26.ZEBOV, highlighting the pivotal role of the cell-fate decision at early time points after vaccination in determination of the short- and long-term antibody titers. This confirms the key regulatory role of *HESX1* in the framework of Wnt signaling and in the innate im-

mune response to Ad26.ZEBOV. On day 7, genes correlated with antibody response at day 364 corresponded to B cell and plasma cell responses. The most important markers were represented by *IGHV3\_13*, *IGHV2\_5*, and *IGLV1\_47*. However, we did not identify the IFN-pathway-related gene IP-10 (*CXCL10*) as a best-of-class gene that correlates with the vaccine-induced antibody response, as reported for the early innate immune response to the rVSV-ZEBOV vaccine in humans.<sup>5</sup> Interestingly, both a common prevaccination and an early time-adjusted post-vaccination gene-signature-predicting antibody response were observed across several vaccines,<sup>82,100</sup> demonstrating that variations in the transcriptional state of the innate immune response can be an essential determinant of responsiveness to vaccination. Overall, our study identified genes committed to the immune response to the Ad26.ZEBOV vaccine, which strengthens our understanding of viral-vector vaccine mechanisms. Finally, our predictive genes of antibody responses remain to be validated on other vaccines. The identification of molecules of vaccine responsiveness provides new targets to modulate for increasing the effectiveness of vaccines.

#### Limitations of the study

This study had limitations. We used RNA sequencing data to infer cell composition in blood at days 1 and 7 after the first injection of the vaccine, without confirmation of the cell population based on cell phenotypic analysis. One limitation was the lack of information about Ad26 vector-specific antibody titers before vaccination in volunteers included in this trial. Therefore, we could not discriminate responses against the vector and the Ad26.ZEBOV. Likewise, the absence of a control group receiving blank viral vector injection did not allow us to make a comparison with the response stimulated by Ebola virus GP in viral vectors.

#### STAR★METHODS

Detailed methods are provided in the online version of this paper and include the following:

- KEY RESOURCES TABLE
- RESOURCE AVAILABILITY
  - Lead contact
  - Materials availability
  - Data and code availability
- EXPERIMENTAL MODEL AND STUDY PARTICIPANT DETAILS
  - Study participants and samples
- METHOD DETAILS
  - Assessment of ebola virus GP binding antibody concentrations
  - RNA extraction, library preparation, and sequencing
  - Differential gene expression analysis
  - Cell deconvolution analysis
  - Construction of a protein-protein interactions (PPI) network
  - Molecular Complex Detection (MCODE) and identification

- Identification of DEGs correlating with antibody response after MVA-BN-FILO injection
- Heatmap
- **QUANTIFICATION AND STATISTICAL ANALYSIS**

#### SUPPLEMENTAL INFORMATION

Supplemental information can be found online at <https://doi.org/10.1016/j.celrep.2023.113101>.

#### ACKNOWLEDGMENTS

The study was coordinated by the EBOVAC2 multi-partner research consortium, which received funding from the Innovative Medicines Initiative 2 Joint Undertaking (grant no. 115861) as part of the IMI Ebola+ program. This Joint Undertaking receives support from the EU's Horizon 2020 Framework Programme for Research and Innovation and the European Federation of Pharmaceutical Industries and Associations. The EBOVAC2 members include Janssen Vaccines & Prevention BV, which is part of the Janssen Pharmaceutical Companies of Johnson & Johnson (the study sponsor), the Centre Muraz, INSERM, INSERM Transfert SA, the London School of Hygiene & Tropical Medicine, and the University of Oxford. The authors acknowledge the contribution of all participants who took part in the studies; the partners of the EBOVAC2 consortium, including INSERM, the London School of Hygiene & Tropical Medicine, the University of Oxford, the Center Muraz, and INSERM Transfert; the members of the Scientific Advisory Board, David Kraslow, Abdel Babiker, and Nigel Klein; the members of the Ethical Advisory Board; and the members of the Data Safety Monitoring Board, John Bruce McClain, Marie-Louise Newell, and Geert Molenberghs. This work was also supported by the Vaccine Research Institute (VRI), managed by the ANR under reference ANR-10-LABX-77-01 and the EBOVAC2 project. Funding sources were not involved in the study design, data acquisition, data analysis, data interpretation, or writing of the manuscript.

#### AUTHOR CONTRIBUTIONS

Y.L., R.T., L.R., and H.H. designed the study. F.B., C.L., and P.T. participated in sample data collection. C.L., P.T., and F.B. performed the experiments. H.H., F.B., L.R., Y.L., C.M., K.L., M.D., B.H., and R.T. analyzed and interpreted the data. H.H., F.B., L.R., R.T., and Y.L. drafted the first version and wrote the final version of the manuscript. All authors approved the final version.

#### DECLARATION OF INTERESTS

The authors declare no competing interests.

Received: April 11, 2023

Revised: July 24, 2023

Accepted: August 21, 2023

Published: September 8, 2023

#### REFERENCES

1. Hensley, L.E., Jones, S.M., Feldmann, H., Jahrling, P.B., and Geisbert, T.W. (2005). Ebola and Marburg viruses: pathogenesis and development of countermeasures. *Curr. Mol. Med.* *5*, 761–772. <https://doi.org/10.2174/156652405774962344>.
2. Henao-Restrepo, A.M., Camacho, A., Longini, I.M., Watson, C.H., Edmunds, W.J., Egger, M., Carroll, M.W., Dean, N.E., Diatta, I., Doumbia, M., et al. (2017). Efficacy and effectiveness of an rVSV-vectored vaccine in preventing Ebola virus disease: final results from the Guinea ring vaccination, open-label, cluster-randomised trial (Ebola Ça Suffit!). *Lancet* *389*, 505–518. PDF. [https://doi.org/10.1016/S0140-6736\(16\)32621-6/ATTACHMENT/BDS27270-BD02-432A-85F7-C645BE8108C8/MMC1](https://doi.org/10.1016/S0140-6736(16)32621-6/ATTACHMENT/BDS27270-BD02-432A-85F7-C645BE8108C8/MMC1).
3. Lévy, Y., Lane, C., Piot, P., Beavogui, A.H., Kieh, M., Leigh, B., Doumbia, S., D'Ortenzio, E., Lévy-Marchal, C., Pierson, J., et al. (2018). Prevention of Ebola virus disease through vaccination: where we are in 2018. *Lancet* *392*, 787–790. [https://doi.org/10.1016/S0140-6736\(18\)31710-0](https://doi.org/10.1016/S0140-6736(18)31710-0).
4. Huttner, A., Combescure, C., Grillet, S., Haks, M.C., Quinten, E., Modoux, C., Agnandji, S.T., Brosnahan, J., Daye, J.A., Harandi, A.M., et al. (2017). A dose-dependent plasma signature of the safety and immunogenicity of the rVSV-Ebola vaccine in Europe and Africa. *Sci. Transl. Med.* *9*, eaaj1701. [https://doi.org/10.1126/SCITRANSLMED.AAJ1701/SUPPL\\_FILE/AJ1701\\_SM.PDF](https://doi.org/10.1126/SCITRANSLMED.AAJ1701/SUPPL_FILE/AJ1701_SM.PDF).
5. Rechten, A., Richert, L., Lorenzo, H., Martrus, G., Hejblum, B., Dahlke, C., Kasonta, R., Zinser, M., Stubbe, H., Matschl, U., et al. (2017). Systems Vaccinology Identifies an Early Innate Immune Signature as a Correlate of Antibody Responses to the Ebola Vaccine rVSV-ZEBOV. *Cell Rep.* *20*, 2251–2261. <https://doi.org/10.1016/j.celrep.2017.08.023>.
6. Medagliani, D., Santoro, F., and Siegrist, C.A. (2018). Correlates of vaccine-induced protective immunity against Ebola virus disease. *Semin. Immunol.* *39*, 65–72. <https://doi.org/10.1016/J.SMIM.2018.07.003>.
7. Callendret, B., Vellinga, J., Wunderlich, K., Rodriguez, A., Steigerwald, R., Dirmeier, U., Cheminay, C., Volkmann, A., Brasel, T., Carrion, R., et al. (2018). A prophylactic multivalent vaccine against different filovirus species is immunogenic and provides protection from lethal infections with Ebolavirus and Marburgvirus species in non-human primates. *PLoS One* *13*, e0192312. <https://doi.org/10.1371/JOURNAL.PONE.0192312>.
8. Milligan, I.D., Gibani, M.M., Sewell, R., Clutterbuck, E.A., Campbell, D., Plested, E., Nuthall, E., Voysey, M., Silva-Reyes, L., McElrath, M.J., et al. (2016). Safety and immunogenicity of novel adenovirus type 26-and modified vaccinia Ankara-vectored Ebola vaccines: A randomized clinical trial. *JAMA* *315*, 1610–1623. <https://doi.org/10.1001/jama.2016.4218>.
9. Bejjani, F., Evanno, E., Zibara, K., Piechaczyk, M., and Jariel-Encontre, I. (2019). The AP-1 transcriptional complex: Local switch or remote command? *Biochim. Biophys. Acta Rev. Canc* *1872*, 11–23. <https://doi.org/10.1016/j.bbcan.2019.04.003>.
10. Winslow, R.L., Milligan, I.D., Voysey, M., Luhn, K., Shukarev, G., Douoguih, M., and Snape, M.D. (2017). Immune Responses to Novel Adenovirus Type 26 and Modified Vaccinia Virus Ankara-Vectored Ebola Vaccines at 1 Year. *JAMA* *317*, 1075–1077. <https://doi.org/10.1001/JAMA.2016.20644>.
11. Anywaine, Z., Barry, H., Anzala, O., Mutua, G., Sirima, S.B., Eholie, S., Kibuuka, H., Bétard, C., Richert, L., Lacabaratz, C., et al. (2022). Safety and immunogenicity of 2-dose heterologous Ad26.ZEBOV, MVA-BN-Filo Ebola vaccination in children and adolescents in Africa: A randomised, placebo-controlled, multicentre Phase II clinical trial. *PLoS Med.* *19*, e1003865. <https://doi.org/10.1371/JOURNAL.PMED.1003865>.
12. Anywaine, Z., Whitworth, H., Kaleebu, P., Praygod, G., Shukarev, G., Manno, D., Kapiga, S., Grosskurth, H., Kalluvya, S., Bockstal, V., et al. (2019). Safety and Immunogenicity of a 2-Dose Heterologous Vaccination Regimen with Ad26.ZEBOV and MVA-BN-Filo Ebola Vaccines: 12-Month Data from a Phase 1 Randomized Clinical Trial in Uganda and Tanzania. *J. Infect. Dis.* *220*, 46–56. <https://doi.org/10.1093/infdis/jiz070>.
13. Mutua, G., Anzala, O., Luhn, K., Robinson, C., Bockstal, V., Anumendem, D., and Douoguih, M. (2019). Safety and Immunogenicity of a 2-Dose Heterologous Vaccine Regimen With Ad26.ZEBOV and MVA-BN-Filo Ebola Vaccines: 12-Month Data From a Phase 1 Randomized Clinical Trial in Nairobi, Kenya. *J. Infect. Dis.* *220*, 57–67. <https://doi.org/10.1093/INFDIS/JIZ071>.
14. Goldstein, N., Bockstal, V., Bart, S., Luhn, K., Robinson, C., Gaddah, A., Callendret, B., and Douoguih, M. (2022). Safety and Immunogenicity of Heterologous and Homologous Two Dose Regimens of Ad26- and MVA-Vectored Ebola Vaccines: A Randomized, Controlled Phase 1 Study. *J. Infect. Dis.* *226*, 595–607. <https://doi.org/10.1093/INFDIS/JIAA586>.
15. Barry, H., Mutua, G., Kibuuka, H., Anywaine, Z., Sirima, S.B., Meda, N., Anzala, O., Eholie, S., Bétard, C., Richert, L., et al. (2021). Safety and

- immunogenicity of 2-dose heterologous Ad26.ZEBOV, MVA-BN-Filo Ebola vaccination in healthy and HIV-infected adults: A randomised, placebo-controlled Phase II clinical trial in Africa. *PLoS Med.* 18, e1003813. <https://doi.org/10.1371/JOURNAL.PMED.1003813>.
16. Pollard, A.J., Launay, O., Lelievre, J.D., Lacabartz, C., Grande, S., Goldstein, N., Robinson, C., Gaddah, A., Bockstal, V., Wiedemann, A., et al. (2021). Safety and immunogenicity of a two-dose heterologous Ad26.ZEBOV and MVA-BN-Filo Ebola vaccine regimen in adults in Europe (EBOVAC2): a randomised, observer-blind, participant-blind, placebo-controlled, phase 2 trial. *Lancet Infect. Dis.* 21, 493–506. [https://doi.org/10.1016/S1473-3099\(20\)30476-X](https://doi.org/10.1016/S1473-3099(20)30476-X).
  17. Balelli, I., Pasin, C., Prague, M., Crauste, F., Effelterre, T.V., Bockstal, V., Solforosi, L., and Thiébaud, R. (2020). A model for establishment, maintenance and reactivation of the immune response after vaccination against Ebola virus. *J. Theor. Biol.* 495, 110254. <https://doi.org/10.1016/j.jtbi.2020.110254>.
  18. Pasin, C., Balelli, I., Van Effelterre, T., Bockstal, V., Solforosi, L., Prague, M., Douoguih, M., and Thiébaud, R. (2019). Dynamics of the Humoral Immune Response to a Prime-Boost Ebola Vaccine: Quantification and Sources of Variation. *J. Virol.* 93, e00579-19. <https://doi.org/10.1128/jvi.00579-19>.
  19. Roozendaal, R., Hendriks, J., van Effelterre, T., Spiessens, B., Dekking, L., Solforosi, L., Czapska-Casey, D., Bockstal, V., Stoop, J., Splinter, D., et al. (2020). Nonhuman primate to human immunobridging to infer the protective effect of an Ebola virus vaccine candidate. *NPJ vaccines* 5, 112. <https://doi.org/10.1038/s41541-020-00261-9>.
  20. Gunn, B.M., McNamara, R.P., Wood, L., Taylor, S., Devadhasan, A., Guo, W., Das, J., Nilsson, A., Shurtleff, A., Dubey, S., et al. (2023). Antibodies against the Ebola virus soluble glycoprotein are associated with long-term vaccine-mediated protection of non-human primates. *Cell Rep.* 42, 112402. <https://doi.org/10.1016/j.celrep.2023.112402>.
  21. Wagstaffe, H.R., Anzala, O., Kibuuka, H., Anywaine, Z., Sirima, S.B., Thiébaud, R., Richert, L., Levy, Y., Lacabartz, C., Bockstal, V., et al. (2022). NK Cell Subset Redistribution and Antibody Dependent Activation after Ebola Vaccination in Africans. *Vaccines* 10, 884. <https://doi.org/10.3390/VACCINES10060884>.
  22. Wagstaffe, H.R., Susannini, G., Thiébaud, R., Richert, L., Lévy, Y., Bockstal, V., Stoop, J.N., Luhn, K., Douoguih, M., Riley, E.M., et al. (2021). Durable natural killer cell responses after heterologous two-dose Ebola vaccination. *NPJ vaccines* 6, 19. <https://doi.org/10.1038/S41541-021-00280-0>.
  23. Querec, T.D., Akondy, R.S., Lee, E.K., Cao, W., Nakaya, H.I., Teuwen, D., Pirani, A., Gernert, K., Deng, J., Marzolf, B., et al. (2009). Systems biology approach predicts immunogenicity of the yellow fever vaccine in humans. *Nat. Immunol.* 10, 116–125. <https://doi.org/10.1038/ni.1688>.
  24. Kazmin, D., Nakaya, H.I., Lee, E.K., Johnson, M.J., van der Most, R., van den Berg, R.A., Ballou, W.R., Jongert, E., Wille-Reece, U., Ockenhouse, C., et al. (2017). Systems analysis of protective immune responses to RTS,S malaria vaccination in humans. *Proc. Natl. Acad. Sci. USA* 114, 2425–2430. <https://doi.org/10.1073/pnas.1621489114>.
  25. Nakaya, H.I., Hagan, T., Duraisingham, S.S., Lee, E.K., Kwissa, M., Rouphael, N., Frasca, D., Gersten, M., Mehta, A.K., Gaujoux, R., et al. (2015). Systems Analysis of Immunity to Influenza Vaccination across Multiple Years and in Diverse Populations Reveals Shared Molecular Signatures. *Immunity* 43, 1186–1198. <https://doi.org/10.1016/J.IMMUNI.2015.11.012>.
  26. Nakaya, H.I., Wrammert, J., Lee, E.K., Racioppi, L., Marie-Kunze, S., Haining, W.N., Means, A.R., Kasturi, S.P., Khan, N., Li, G.-M., et al. (2011). Systems biology of vaccination for seasonal influenza in humans. *Nat. Immunol.* 12, 786–795. <https://doi.org/10.1038/ni.2067>.
  27. Popper, S.J., Strouts, F.R., Lindow, J.C., Cheng, H.K., Montoya, M., Balmaseda, A., Durbin, A.P., Whitehead, S.S., Harris, E., Kirkpatrick, B.D., and Relman, D.A. (2018). Early Transcriptional Responses After Dengue Vaccination Mirror the Response to Natural Infection and Predict Neutralizing Antibody Titers. *J. Infect. Dis.* 218, 1911–1921. <https://doi.org/10.1093/INFDIS/JIY434>.
  28. Santoro, F., Donato, A., Lucchesi, S., Sorgi, S., Gerlini, A., Haks, M.C., Ottenhoff, T.H.M., Gonzalez-Dias, P., Consortium, V.E., Consortium, V.E., et al. (2021). Human transcriptomic response to the VSV-vectored ebola vaccine. *Vaccines* 9, 67–15. <https://doi.org/10.3390/vaccines9020067>.
  29. Vianello, E., Gonzalez-Dias, P., van Veen, S., Engele, C.G., Quinten, E., Monath, T.P., Medagliani, D., Agnandij, S.T., Ahmed, R., Anderson, J., et al. (2022). Transcriptomic signatures induced by the Ebola virus vaccine rVSVΔG-ZEBOV-GP in adult cohorts in Europe, Africa, and North America: a molecular biomarker study. *The Lancet Microbe* 3, e113–e123. [https://doi.org/10.1016/S2666-5247\(21\)00235-4/ATTACHMENT/F5D9D3F2-6325-478B-8218-3412EA966A89/MMC9.XLSX](https://doi.org/10.1016/S2666-5247(21)00235-4/ATTACHMENT/F5D9D3F2-6325-478B-8218-3412EA966A89/MMC9.XLSX).
  30. Pasin, C., Balelli, I., Effelterre, T.V., Bockstal, V., Solforosi, L., Prague, M., Douoguih, M., and Thiébaud, R. (2019). Dynamics of the Humoral Immune Response to a Prime-Boost Ebola Vaccine: Quantification and Sources of Variation. *J. Virol.* 93, 579–598. <https://doi.org/10.1128/JVI.00579-19>.
  31. Gauthier, M., Agniel, D., Thiébaud, R., and Hejblum, B.P. (2020). dearseq: a variance component score test for RNA-seq differential analysis that effectively controls the false discovery rate. *NAR Genom. Bioinform.* 2, lqaa093. <https://doi.org/10.1093/NARGAB/LQAA093>.
  32. Batista, N.V., Chang, Y.-H., Chu, K.-L., Wang, K.C., Girard, M., and Watts, T.H. (2020). T Cell-Intrinsic CX3CR1 Marks the Most Differentiated Effector CD4 + T Cells, but Is Largely Dispensable for CD4 + T Cell Responses during Chronic Viral Infection. *ImmunoHorizons* 4, 701–712. <https://doi.org/10.4049/IMMUNOHORIZONS.2000059>.
  33. Bender, A.T., Tzvetkov, E., Pereira, A., Wu, Y., Kasar, S., Przetak, M.M., Vlach, J., Niewold, T.B., Jensen, M.A., and Okitsu, S.L. (2020). TLR7 and TLR8 Differentially Activate the IRF and NF-κB Pathways in Specific Cell Types to Promote Inflammation. *ImmunoHorizons* 4, 93–107. <https://doi.org/10.4049/IMMUNOHORIZONS.2000002>.
  34. Roe, K., Shu, G.L., Draves, K.E., Giordano, D., Pepper, M., and Clark, E.A. (2019). Targeting antigens to CD180 but not CD40 programs immature and mature B cell subsets to become efficient antigen-presenting cells. *J. Immunol.* 203, 1715–1729. <https://doi.org/10.4049/JIMMUNOL.1900549>.
  35. Mola, S., Foisy, S., Boucher, G., Major, F., Beauchamp, C., Karaky, M., Goyette, P., Lesage, S., and Rioux, J.D. (2020). A transcriptome-based approach to identify functional modules within and across primary human immune cells. *PLoS One* 15, e0233543. <https://doi.org/10.1371/JOURNAL.PONE.0233543>.
  36. Goh, S.H., Lee, Y.T., Bhanu, N.V., Cam, M.C., Desper, R., Martin, B.M., Moharram, R., Gherman, R.B., and Miller, J.L. (2005). A newly discovered human α-globin gene. *Blood* 106, 1466–1472. <https://doi.org/10.1182/BLOOD-2005-03-0948>.
  37. Yang, C., Hashimoto, M., Lin, Q.X.X., Tan, D.Q., and Suda, T. (2019). Sphingosine-1-phosphate signaling modulates terminal erythroid differentiation through the regulation of mitophagy. *Exp. Hematol.* 72, 47–59.e1. <https://doi.org/10.1016/J.EXPHEM.2019.01.004>.
  38. Yang, L.V., Wan, J., Ge, Y., Fu, Z., Kim, S.-Y., Fujiwara, Y., Taub, J.W., Matherly, L.H., Eliason, J., and Li, L. (2006). The GATA site-dependent hemogen promoter is transcriptionally regulated by GATA1 in hematopoietic and leukemia cells. *Leukemia* 20, 417–425. <https://doi.org/10.1038/SJ.LEU.2404105>.
  39. Morera, D., and MacKenzie, S.A. (2011). Is there a direct role for erythrocytes in the immune response? *Vet. Res.* 42, 89. <https://doi.org/10.1186/1297-9716-42-89>.
  40. Anderson, H.L., Brodsky, I.E., and Mangalmurti, N.S. (2018). The Evolving Erythrocyte: Red Blood Cells as Modulators of Innate Immunity. *J. Immunol.* 201, 1343–1351. <https://doi.org/10.4049/jimmunol.1800565>.

41. Pretini, V., Koenen, M.H., Kaestner, L., Fens, M.H.A.M., Schifferers, R.M., Bartels, M., and Van Wijk, R. (2019). Red Blood Cells: Chasing Interactions. *Front. Physiol.* *10*, 945. <https://doi.org/10.3389/fphys.2019.00945>.
42. Walsh, D. (2010). Manipulation of the host translation initiation complex eIF4F by DNA viruses. *Biochem. Soc. Trans.* *38*, 1511–1516. <https://doi.org/10.1042/bst0381511>.
43. Sadler, A.J., Latchoumanin, O., Hawkes, D., Mak, J., and Williams, B.R.G. (2009). An antiviral response directed by PKR phosphorylation of the RNA helicase A. *PLoS Pathog.* *5*, e1000311. <https://doi.org/10.1371/JOURNAL.PPAT.1000311>.
44. Burgess, H.M., and Mohr, I. (2015). Cellular 5'-3' mRNA exonuclease Xrn1 controls double-stranded RNA accumulation and anti-viral responses. *Cell Host Microbe* *17*, 332–344. <https://doi.org/10.1016/j.chom.2015.02.003>.
45. Wong, J.J.Y., Pung, Y.F., Sze, N.S.-K., and Chin, K.-C. (2006). HERC5 is an IFN-induced HECT-type E3 protein ligase that mediates type I IFN-induced ISGylation of protein targets. *Proc. Natl. Acad. Sci. USA* *103*, 10735–10740. <https://doi.org/10.1073/PNAS.0600397103>.
46. Griffin, D.E. (2008). Cytokines and Chemokines. *Encyclopedia of Virology*, 620–624. <https://doi.org/10.1016/B978-012374410-4.00374-5>.
47. Zhang, Q., Putheti, P., Zhou, Q., Liu, Q., and Gao, W. (2008). Structures and biological functions of IL-31 and IL-31 receptors. *Cytokine Growth Factor Rev.* *19*, 347–356. <https://doi.org/10.1016/J.CYTOGFR.2008.08.003>.
48. Datsi, A., Steinhoff, M., Ahmad, F., Alam, M., and Buddenkotte, J. (2021). Interleukin-31: The “itchy” cytokine in inflammation and therapy. *Allergy* *76*, 2982–2997. <https://doi.org/10.1111/ALL.14791>.
49. Bournazos, S., Gupta, A., and Ravetch, J.V. (2020). The role of IgG Fc receptors in antibody-dependent enhancement. *Nat. Rev. Immunol.* *20*, 633–643. <https://doi.org/10.1038/s41577-020-00410-0>.
50. Di Domizio, J., Blum, A., Gallagher-Gambarelli, M., Molens, J.P., Chaperot, L., and Plumas, J. (2009). TLR7 stimulation in human plasmacytoid dendritic cells leads to the induction of early IFN-inducible genes in the absence of type I IFN. *Blood* *114*, 1794–1802. <https://doi.org/10.1182/BLOOD-2009-04-216770>.
51. Silverstein, R.L., and Febbraio, M. (2009). CD36, a scavenger receptor involved in immunity, metabolism, angiogenesis, and behavior. *Sci. Signal.* *2*, re3. <https://doi.org/10.1126/SCISIGNAL.272RE3>.
52. Maler, M.D., Nielsen, P.J., Stichling, N., Cohen, I., Ruzsics, Z., Wood, C., Engelhard, P., Suomalainen, M., Gyory, I., Huber, M., et al. (2017). Key Role of the Scavenger Receptor MARCO in Mediating Adenovirus Infection and Subsequent Innate Responses of Macrophages. *mBio* *8*, e00670-17. <https://doi.org/10.1128/MBIO.00670-17>.
53. Patten, D.A. (2018). SCARF1: a multifaceted, yet largely understudied, scavenger receptor. *Inflamm. Res.* *67*, 627–632. <https://doi.org/10.1007/S00011-018-1154-7>.
54. Honarmand Ebrahimi, K. (2018). A unifying view of the broad-spectrum antiviral activity of RSAD2 (viperin) based on its radical-SAM chemistry. *Metallomics* *10*, 539–552. <https://doi.org/10.1039/C7MT00341B>.
55. Li, Y., Banerjee, S., Wang, Y., Goldstein, S.A., Dong, B., Gaughan, C., Silverman, R.H., and Weiss, S.R. (2016). Activation of RNase L is dependent on OAS3 expression during infection with diverse human viruses. *Proc. Natl. Acad. Sci. USA* *113*, 2241–2246. <https://doi.org/10.1073/pnas.1519657113>.
56. Mathieu, N.A., Papparisto, E., Barr, S.D., and Spratt, D.E. (2021). HERC5 and the ISGylation Pathway: Critical Modulators of the Antiviral Immune Response. *Viruses* *13*, 1102. <https://doi.org/10.3390/V13061102>.
57. Bilir, C., and Sarisozen, C. (2017). Indoleamine 2,3-dioxygenase (IDO): Only an enzyme or a checkpoint controller? *Journal of Oncological Sciences* *3*, 52–56. <https://doi.org/10.1016/J.JONS.2017.04.001>.
58. Haneda, T., Imai, Y., Uchiyama, R., Jitsukawa, O., and Yamanishi, K. (2016). Activation of Molecular Signatures for Antimicrobial and Innate Defense Responses in Skin with Transglutaminase 1 Deficiency. *PLoS One* *11*, e0159673. <https://doi.org/10.1371/journal.pone.0159673>.
59. Fabrizio, F.P., Trombetta, D., Rossi, A., Sparaneo, A., Castellana, S., and Muscarella, L.A. (2018). Gene code CD274/PD-L1: from molecular basis toward cancer immunotherapy. *Ther. Adv. Med. Oncol.* *10*, 1758835918815598. <https://doi.org/10.1177/1758835918815598>.
60. Andoniadou, C.L., Signore, M., Young, R.M., Gaston-Massuet, C., Wilson, S.W., Fuchs, E., and Martinez-Barbera, J.P. (2011). HESX1- and TCF3-mediated repression of Wnt/ $\beta$ -catenin targets is required for normal development of the anterior forebrain. *Development* *138*, 4931–4942. <https://doi.org/10.1242/dev.066597>.
61. Aksoy, E., Albarani, V., Nguyen, M., Laes, J.F., Ruelle, J.L., De Wit, D., Willems, F., Goldman, M., and Goriely, S. (2007). Interferon regulatory factor 3-dependent responses to lipopolysaccharide are selectively blunted in cord blood cells. *Blood* *109*, 2887–2893. <https://doi.org/10.1182/blood-2006-06-027862>.
62. Gilchrist, M., Thorsson, V., Li, B., Rust, A.G., Korb, M., Roach, J.C., Kennedy, K., Hai, T., Bolouri, H., and Aderem, A. (2006). Systems biology approaches identify ATF3 as a negative regulator of Toll-like receptor 4. *Nature* *441*, 173–178. <https://doi.org/10.1038/nature04768>.
63. Bin, L., Li, X., Feng, J., Richers, B., and Leung, D.Y. (2016). Ankyrin Repeat Domain 22 Mediates Host Defense Against Viral Infection Through STING Signaling Pathway. *J. Immunol.* *196*, 201.4.
64. Froggatt, H.M., Harding, A.T., Chaparian, R.R., and Heaton, N.S. (2021). ETV7 limits antiviral gene expression and control of influenza viruses. *Sci. Signal.* *14*, eabe1194. <https://doi.org/10.1126/scisignal.abe1194>.
65. Papavassiliou, A.G., and Musti, A.M. (2020). The Multifaceted Output of c-Jun Biological Activity: Focus at the Junction of CD8 T Cell Activation and Exhaustion. *Cells* *9*. <https://doi.org/10.3390/CELLS9112470>.
66. Rasighaemi, P., and Ward, A.C. (2017). ETV6 and ETV7: Siblings in hematopoiesis and its disruption in disease. *Crit. Rev. Oncol. Hematol.* *116*, 106–115. <https://doi.org/10.1016/j.critrevonc.2017.05.011>.
67. Cassandri, M., Smirnov, A., Novelli, F., Pitolli, C., Agostini, M., Malewicz, M., Melino, G., and Raschella, G. (2017). Zinc-finger proteins in health and disease. *Cell Death Dis.* *3*, 17071–17112. <https://doi.org/10.1038/cddiscovery.2017.71>.
68. Tsuji, S., Cortesão, C., Bram, R.J., Platt, J.L., and Cascalho, M. (2011). TACI deficiency impairs sustained Blimp-1 expression in B cells decreasing long-lived plasma cells in the bone marrow. *Blood* *118*, 5832–5839. <https://doi.org/10.1182/blood-2011-05-353961>.
69. Shah, N., Chari, A., Scott, E., Mezzi, K., and Usmani, S.Z. (2020). B-cell maturation antigen (BCMA) in multiple myeloma: rationale for targeting and current therapeutic approaches. *Leukemia* *34*, 985–1005. <https://doi.org/10.1038/s41375-020-0734-z>.
70. Glaría, E., and Valledor, A.F. (2020). Roles of CD38 in the Immune Response to Infection. *Cells* *9*. <https://doi.org/10.3390/CELLS9010228>.
71. Choi, J., Phelan, J.D., Wright, G.W., Häupl, B., Huang, D.W., Shaffer, A.L., Young, R.M., Wang, Z., Zhao, H., Yu, X., et al. (2020). Regulation of B cell receptor-dependent NF- $\kappa$ B signaling by the tumor suppressor KLHL14. *Proceedings of the National Academy of Sciences of the United States of America* *117*, 6092–6102. [https://doi.org/10.1073/PNAS.1921187117/SUPPL\\_FILE/PNAS.1921187117.SD05.XLSX](https://doi.org/10.1073/PNAS.1921187117/SUPPL_FILE/PNAS.1921187117.SD05.XLSX).
72. Newman, A.M., Liu, C.L., Green, M.R., Gentles, A.J., Feng, W., Xu, Y., Hoang, C.D., Diehn, M., and Alizadeh, A.A. (2015). Robust enumeration of cell subsets from tissue expression profiles. *Nat. Methods* *12*, 453–457. <https://doi.org/10.1038/nmeth.3337>.
73. Wang, Z., Zhang, H., and Cheng, Q. (2020). PDIA4: The basic characteristics, functions and its potential connection with cancer. *Biomed. Pharmacother.* *122*, 109688. <https://doi.org/10.1016/J.BIOPHA.2019.109688>.
74. Liu, B., and Li, Z. (2008). Endoplasmic reticulum HSP90 $\beta$  (gp96, grp94) optimizes B-cell function via chaperoning integrin and TLR but not immunoglobulin. *Blood* *112*, 1223–1230. <https://doi.org/10.1182/blood-2008-03-143107>.

75. Jumaa, H., Caganova, M., McAllister, E.J., Hoenig, L., He, X., Saltukoglu, D., Brenker, K., Köhler, M., Leben, R., Hauser, A.E., et al. (2020). Immunoglobulin expression in the endoplasmic reticulum shapes the metabolic fitness of B lymphocytes. *Life Sci. Alliance* 3, e202000700. <https://doi.org/10.26508/LSA.202000700>.
76. Ehrhardt, S.A., Zehner, M., Krähling, V., Cohen-Dvashi, H., Kreer, C., Elad, N., Gruell, H., Ercanoglu, M.S., Schommers, P., Giesemann, L., et al. (2019). Polyclonal and convergent antibody response to Ebola virus vaccine rVSV-ZEBOV. *Nat. Med.* 25, 1589–1600. <https://doi.org/10.1038/S41591-019-0602-4>.
77. Cagigi, A., Misasi, J., Ploquin, A., Stanley, D.A., Ambrozak, D., Tsybovsky, Y., Mason, R.D., Roederer, M., and Sullivan, N.J. (2018). Vaccine Generation of Protective Ebola Antibodies and Identification of Conserved B-Cell Signatures. *J. Infect. Dis.* 218, S528–S536. <https://doi.org/10.1093/infdis/jiy333>.
78. Logue, J., Tuznik, K., Follmann, D., Grandits, G., Marchand, J., Reilly, C., Sarro, Y.D.S., Pettitt, J., Stavale, E.J., Fallah, M., et al. (2018). Use of the Filovirus Animal Non-Clinical Group (FANG) Ebola virus immuno-assay requires fewer study participants to power a study than the Alpha Diagnostic International assay. *J. Virol. Methods* 255, 84–90. <https://doi.org/10.1016/j.jviromet.2018.02.018>.
79. Kennedy, S.B., Bolay, F., Kieh, M., Grandits, G., Badio, M., Ballou, R., Eckes, R., Feinberg, M., Follmann, D., Grund, B., et al. (2017). Phase 2 Placebo-Controlled Trial of Two Vaccines to Prevent Ebola in Liberia. *N. Engl. J. Med.* 377, 1438–1447. <https://doi.org/10.1056/NEJMoa1614067>.
80. Tibshirani, R. (1996). Regression Shrinkage and Selection via the Lasso. *J. Roy. Stat. Soc. B* 58, 267–288.
81. Hai, T., Wolford, C.C., and Chang, Y.S. (2010). ATF3, a hub of the cellular adaptive-response network, in the pathogenesis of diseases: is modulation of inflammation a unifying component? *Gene Expr.* 15, 1–11. <https://doi.org/10.3727/105221610X1281968655015>.
82. Hagan, T., Gerritsen, B., Tomalin, L.E., Fourati, S., Mulè, M.P., Chawla, D.G., Rychkov, D., Henrich, E., Miller, H.E.R., Diray-Arce, J., et al. (2022). Transcriptional atlas of the human immune response to 13 vaccines reveals a common predictor of vaccine-induced antibody responses. *Nat. Immunol.* 23, 1788–1798. <https://doi.org/10.1038/s41590-022-01328-6>.
83. Karsten, E., and Herbert, B.R. (2020). The emerging role of red blood cells in cytokine signalling and modulating immune cells. *Blood Rev.* 41, 100644. <https://doi.org/10.1016/j.blre.2019.100644>.
84. Lam, L.K.M., Murphy, S., Kokkinaki, D., Venosa, A., Sherrill-Mix, S., Casu, C., Rivella, S., Weiner, A., Park, J., Shin, S., et al. (2021). DNA binding to TLR9 expressed by red blood cells promotes innate immune activation and anemia. *Sci. Transl. Med.* 13. [https://doi.org/10.1126/SCITRANSLMED.ABJ1008/SUPPL\\_FILE/SCITRANSLMED.ABJ1008\\_DATA\\_FILES\\_S1\\_TO\\_S3.ZIP](https://doi.org/10.1126/SCITRANSLMED.ABJ1008/SUPPL_FILE/SCITRANSLMED.ABJ1008_DATA_FILES_S1_TO_S3.ZIP).
85. Hutnick, N.A., Carnathan, D., Demers, K., Makedonas, G., Ertl, H.C.J., and Betts, M.R. (2010). Adenovirus-Specific Human T cells are Pervasive, Polyfunctional, and Cross Reactive. *Vaccine* 28, 1932–1941. <https://doi.org/10.1016/J.VACCINE.2009.10.091>.
86. Pédrón, B., Guérin, V., Cordeiro, D.J., Masmoudi, S., Dalle, J.H., and Sterkers, G. (2011). Development of Cytomegalovirus and Adenovirus-Specific Memory CD4 T-Cell Functions From Birth to Adulthood. *Pediatr. Res.* 69, 106–111. <https://doi.org/10.1203/pdr.0b013e318204e469>.
87. Nienen, M., Stervbo, U., Mölder, F., Kaliszczyk, S., Kuchenbecker, L., Gayova, L., Schweiger, B., Jürchott, K., Hecht, J., Neumann, A.U., et al. (2019). The role of pre-existing cross-reactive central memory CD4 T-cells in vaccination with previously unseen influenza strains. *Front. Immunol.* 10, 593. <https://doi.org/10.3389/FIMMU.2019.00593/BIBTEX>.
88. Chaplin, J.W., Kasahara, S., Clark, E.A., and Ledbetter, J.A. (2011). Anti-CD180 (RP105) activates B cells to rapidly produce polyclonal Ig via a T cell and MyD88-independent pathway. *J. Immunol.* 187, 4199–4209. <https://doi.org/10.4049/JIMMUNOL.1100198>.
89. Chaplin, J.W., Chappell, C.P., and Clark, E.A. (2013). Targeting antigens to CD180 rapidly induces antigen-specific IgG, affinity maturation, and immunological memory. *J. Exp. Med.* 210, 2135–2146. <https://doi.org/10.1084/JEM.20130188>.
90. Giles, A.R., Calcedo, R., Tretiakova, A.P., and Wilson, J.M. (2020). Isolating Human Monoclonal Antibodies Against Adeno-Associated Virus From Donors With Pre-existing Immunity. *Front. Immunol.* 11, 1135. <https://doi.org/10.3389/FIMMU.2020.01135/FULL>.
91. Hartnell, F., Brown, A., Capone, S., Kopycinski, J., Bliss, C., Makvandi-Nejad, S., Swadling, L., Ghaffari, E., Cicconi, P., Del Sorbo, M., et al. (2018). A novel vaccine strategy employing serologically different chimpanzee adenoviral vectors for the prevention of HIV-1 and HCV coinfection. *Front. Immunol.* 9, 3175. <https://doi.org/10.3389/FIMMU.2018.03175/BIBTEX>.
92. Hou, J., Wang, S., Jia, M., Li, D., Liu, Y., Li, Z., Zhu, H., Xu, H., Sun, M., Lu, L., et al. (2017). A Systems Vaccinology Approach Reveals Temporal Transcriptomic Changes of Immune Responses to the Yellow Fever 17D Vaccine. *J. Immunol.* 199, 1476–1489. <https://doi.org/10.4049/jimmunol.1700083>.
93. Zak, D.E., Andersen-Nissen, E., Peterson, E.R., Sato, A., Hamilton, M.K., Borgerding, J., Krishnamurthy, A.T., Chang, J.T., Adams, D.J., Hensley, T.R., et al. (2012). Merck Ad5/HIV induces broad innate immune activation that predicts CD8+ T-cell responses but is attenuated by preexisting Ad5 immunity. *Proc. Natl. Acad. Sci. USA* 109, E3503–E3512. <https://doi.org/10.1073/PNAS.1208972109>.
94. Yang, E., and Li, M.M.H. (2020). All About the RNA: Interferon-Stimulated Genes That Interfere With Viral RNA Processes. *Front. Immunol.* 11, 605024–613195. <https://doi.org/10.3389/FIMMU.2020.605024>.
95. Li, M.M.H., MacDonald, M.R., and Rice, C.M. (2015). To translate, or not to translate: viral and host mRNA regulation by interferon-stimulated genes. *Trends Cell Biol.* 25, 320–329. <https://doi.org/10.1016/J.TCB.2015.02.001>.
96. Bevington, S.L., Cauchy, P., Piper, J., Bertrand, E., Lalli, N., Jarvis, R.C., Gilding, L.N., Ott, S., Bonifer, C., and Cockerill, P.N. (2016). Inducible chromatin priming is associated with the establishment of immunological memory in T cells. *EMBO J.* 35, 515–535. <https://doi.org/10.15252/embj.201592534>.
97. Wei, Y., Chen, S., Wang, M., and Cheng, A. (2018). Tripartite motif-containing proteins precisely and positively affect host antiviral immune response. *Scand. J. Immunol.* 87, e12669. <https://doi.org/10.1111/SJ.12669>.
98. Gaudette, B.T., Jones, D.D., Bortnick, A., Argon, Y., and Allman, D. (2020). mTORC1 coordinates an immediate unfolded protein response-related transcriptome in activated B cells preceding antibody secretion. *Nat. Commun.* 11, 723–816. <https://doi.org/10.1038/s41467-019-14032-1>.
99. Tang, M., Liao, M., Ai, X., and He, G. (2021). Increased CDCA2 Level Was Related to Poor Prognosis in Hepatocellular Carcinoma and Associated With Up-Regulation of Immune Checkpoints. *Front. Med.* 8, 773724. <https://doi.org/10.3389/fmed.2021.773724>.
100. Fourati, S., Tomalin, L.E., Mulè, M.P., Chawla, D.G., Gerritsen, B., Rychkov, D., Henrich, E., Miller, H.E.R., Hagan, T., Diray-Arce, J., et al. (2022). Pan-vaccine analysis reveals innate immune endotypes predictive of antibody responses to vaccination. *Nat. Immunol.* 23, 1777–1787. <https://doi.org/10.1038/s41590-022-01329-5>.
101. Durinck, S., Spellman, P.T., Birney, E., and Huber, W. (2009). Mapping identifiers for the integration of genomic datasets with the R/Bioconductor package biomaRt. *Nat. Protoc.* 4, 1184–1191. <https://doi.org/10.1038/nprot.2009.97>.
102. Patro, R., Duggal, G., Love, M.I., Irizarry, R.A., and Kingsford, C. (2017). Salmon provides fast and bias-aware quantification of transcript expression. *Nat. Methods* 14, 417–419. <https://doi.org/10.1038/NMETH.4197>.
103. Ewels, P., Magnusson, M., Lundin, S., and Käller, M. (2016). MultiQC: summarize analysis results for multiple tools and samples in a single

- report. *Bioinformatics* 32, 3047–3048. <https://doi.org/10.1093/bioinformatics/btw354>.
104. Yu, G., Wang, L.-G., Han, Y., and He, Q.-Y. (2012). clusterProfiler: an R Package for Comparing Biological Themes Among Gene Clusters. *OMICS A J. Integr. Biol.* 16, 284–287. <https://doi.org/10.1089/OMI.2011.0118>.
105. Wickham, H. (2016). ggplot2: Elegant Graphics for Data Analysis. <https://doi.org/10.1007/978-3-319-24277-4>.
106. Mangiola, S., Molania, R., Dong, R., Doyle, M.A., and Papenfuss, A.T. (2021). tidybulk: an R tidy framework for modular transcriptomic data analysis. *Genome Biol.* 22, 42–15. <https://doi.org/10.1186/S13059-020-02233-7>.
107. Szklarczyk, D., Gable, A.L., Lyon, D., Junge, A., Wyder, S., Huerta-Cepas, J., Simonovic, M., Doncheva, N.T., Morris, J.H., Bork, P., et al. (2019). STRING v11: protein-protein association networks with increased coverage, supporting functional discovery in genome-wide experimental datasets. *Nucleic Acids Res.* 47, D607–d613. <https://doi.org/10.1093/nar/gky1131>.
108. Shannon, P., Markiel, A., Ozier, O., Baliga, N.S., Wang, J.T., Ramage, D., Amin, N., Schwikowski, B., and Ideker, T. (2003). Cytoscape: a software environment for integrated models of biomolecular interaction networks. *Genome Res.* 13, 2498–2504. <https://doi.org/10.1101/gr.1239303>.
109. Bader, G.D., and Hogue, C.W.V. (2003). An automated method for finding molecular complexes in large protein interaction networks. *BMC Bioinf.* 4, 2. <https://doi.org/10.1186/1471-2105-4-2>.
110. Friedman, J., Hastie, T., and Tibshirani, R. (2010). Regularization Paths for Generalized Linear Models via Coordinate Descent. *J. Stat. Software* 33, 1–22.
111. Gu, Z., Eils, R., and Schlesner, M. (2016). Complex heatmaps reveal patterns and correlations in multidimensional genomic data. *Bioinformatics* 32, 2847–2849. <https://doi.org/10.1093/BIOINFORMATICS/BTW313>.
112. Zhou, Y., Zhou, B., Pache, L., Chang, M., Khodabakhshi, A.H., Tanaseichuk, O., Benner, C., and Chanda, S.K. (2019). Metascape provides a biologist-oriented resource for the analysis of systems-level datasets. *Nat. Commun.* 10, 1523. <https://doi.org/10.1038/s41467-019-09234-6>.
113. Simon, N., Friedman, J., Hastie, T., and Tibshirani, R. (2011). Regularization Paths for Cox’s Proportional Hazards Model via Coordinate Descent. *J. Stat. Software* 39, 1–13. <https://doi.org/10.18637/jss.v039.i05>.



## STAR★METHODS

### KEY RESOURCES TABLE

REAGENT or RESOURCE	SOURCE	IDENTIFIER
<b>Biological samples</b>		
Human blood from healthy volunteers	Seven hospitals in France (Creteil, Lyon, Paris, Rennes, Saint-Etienne, Strasbourg, and Tours)	Patient information is available in Table S1
Monovalent Ad26.ZEBOV expressing the GP of the Ebola Zaire virus (Mayinga variant) and multivalent MVA-BN-Filo expressing the GP of the Sudan and Zaire Ebola viruses and Marburg virus, together with Tai Forest virus nucleoprotein	Janssen Vaccines and Prevention B.V., the Netherlands and Bavarian Nordic, Denmark	Johnson and Johnson Zabdeno® vaccine (Ad26. ZEBOV) and Mvabea® vaccine (MVA-BN-Filo)
<b>Critical commercial assays</b>		
Tempus™ Blood RNA tubes	ThermoFisher Scientific	Cat# 4342792
Tempus™ Spin RNA Isolation Kit	ThermoFisher Scientific	Cat# 4380204
GLOBINclear™- Human Kit	Invitrogen	Cat# 10402478
NEBNext single cell/low input RNA library prep kit for Illumina	NEBNext Biolab	Cat# E6420L
Illumina HiSeq SR Cluster Kit v4 cBot	Illumina	Cat# GD-401-4001
Illumina HiSeq SBS Kit v4	Illumina	Cat# FC-401-4002
Ebola virus GP Filovirus Animal Non-Clinical Group ELISA at Q2 Solutions Laboratories	Q2 Solutions Laboratories Pollard et al. <sup>16</sup> Logue et al. <sup>78</sup> Kennedy et al. <sup>79</sup>	Q <sup>2</sup> Solutions Laboratories
<b>Deposited data</b>		
Raw and analyzed data	This paper	The data generated in this publication have been deposited in NCBI's Gene Expression Omnibus and are accessible through GEO: GSE232633. ( <a href="https://www.ncbi.nlm.nih.gov/geo/query/acc.cgi?acc=GSE232633">https://www.ncbi.nlm.nih.gov/geo/query/acc.cgi?acc=GSE232633</a> )
Human reference transcriptome hg18	Genome Reference Consortium Human Build 38	<a href="https://www.ncbi.nlm.nih.gov/assembly/GCF_000001405.26/">https://www.ncbi.nlm.nih.gov/assembly/GCF_000001405.26/</a>
Annotation model "hsapiens_gene_ensembl"	Genome Reference Consortium Human Build 38 on BiomaRt R package	<a href="https://www.ncbi.nlm.nih.gov/assembly/GCF_000001405.26/">https://www.ncbi.nlm.nih.gov/assembly/GCF_000001405.26/</a>
<b>Software and algorithms</b>		
R package biomaRt v2.42.1	Durinck et al. <sup>101</sup>	<a href="https://bioconductor.org/packages/release/bioc/html/biomaRt.html">https://bioconductor.org/packages/release/bioc/html/biomaRt.html</a>
Salmon v0.8.2	Patro et al. <sup>102</sup>	<a href="https://github.com/COMBINE-lab/Salmon">https://github.com/COMBINE-lab/Salmon</a>
MultiQC v1.4	Ewels et al. <sup>103</sup>	<a href="https://github.com/ewels/MultiQC">https://github.com/ewels/MultiQC</a>
Dearseq package	Gauthier et al. <sup>31</sup>	<a href="https://www.ncbi.nlm.nih.gov/pmc/articles/PMC7676475/">https://www.ncbi.nlm.nih.gov/pmc/articles/PMC7676475/</a>
Ingenuity Pathway Analysis	QIAGEN	<a href="https://www.qiagenbioinformatics.com/products/ingenuity-pathway-analysis">https://www.qiagenbioinformatics.com/products/ingenuity-pathway-analysis</a>
Cluster Profiler R package	Yu et al. <sup>104</sup>	<a href="http://bioconductor.org/packages/release/bioc/html/clusterProfiler.html">http://bioconductor.org/packages/release/bioc/html/clusterProfiler.html</a>
ggplot2 R package	Wickham <sup>105</sup>	<a href="https://ggplot2.tidyverse.org">https://ggplot2.tidyverse.org</a>
CIBERSORT- tidybulk package in R Bioconductor	Mangiola <sup>106</sup>	<a href="https://www.bioconductor.org/packages/release/bioc/html/tidybulk.html">https://www.bioconductor.org/packages/release/bioc/html/tidybulk.html</a> <a href="https://cibersortx.stanford.edu/">https://cibersortx.stanford.edu/</a>
STRING database v11.5	Szklarczyk et al. <sup>107</sup>	<a href="http://string-db.org">http://string-db.org</a>
Cytoscape version 3.8.2	Shannon et al. <sup>108</sup>	<a href="https://cytoscape.org/">https://cytoscape.org/</a>

(Continued on next page)

**Continued**

REAGENT or RESOURCE	SOURCE	IDENTIFIER
MCODE Cytoscape App	Bader et al. <sup>109</sup>	<a href="https://apps.cytoscape.org/apps/mcode">https://apps.cytoscape.org/apps/mcode</a>
glmnet R package v.4.2.6	Friedman et al. <sup>110</sup>	<a href="https://cran.r-hub.io/web/packages/glmnet/index.html">https://cran.r-hub.io/web/packages/glmnet/index.html</a>
Complexheatmap v.2.2.0	Gu et al. <sup>111</sup>	<a href="https://jokergoo.github.io/ComplexHeatmap-reference/book/">https://jokergoo.github.io/ComplexHeatmap-reference/book/</a>
Metascape	Zhou et al. <sup>112</sup>	<a href="https://metascape.org">https://metascape.org</a>

**RESOURCE AVAILABILITY**

**Lead contact**

Further information and requests for resources and reagents should be directed to and will be fulfilled by the corresponding author, Yves Lévy ([yves.levy@aphp.fr](mailto:yves.levy@aphp.fr)).

**Materials availability**

This study did not generate new unique materials.

**Data and code availability**

- The RNA-Sequencing data generated in this publication have been deposited in NCBI's Gene Expression Omnibus and are accessible through GEO Series accession number GSE232633 (<https://www.ncbi.nlm.nih.gov/geo/query/acc.cgi?acc=GSE232633>).
- This paper does not report original code.
- Any additional information required to reanalyze the data reported in this paper is available from the [lead contact](#) upon request.

**EXPERIMENTAL MODEL AND STUDY PARTICIPANT DETAILS**

Eligible, healthy adult volunteers were recruited into a multi-centre, randomised, placebo-controlled, observer blind Ebola vaccine trial, held in Europe; EBL2001 ([ClinicalTrials.gov](https://clinicaltrials.gov) Identifier NCT02416453; registered 15th April 2015, <https://clinicaltrials.gov/ct2/show/NCT02416453?term=VAC52150EBL2001&draw=2&rank=2>). Age, sex and ethnicity of the volunteers are indicated in the supplemental [Table 1](#).

**Study participants and samples**

This observed-blind, phase 2, randomized, placebo-controlled trial was conducted in seven hospitals in France (Creteil, Lyon, Paris, Rennes, Saint-Etienne, Strasbourg, and Tours) and two sites in the UK. Healthy adults aged 18 to 65 years received an injection with monovalent Ad26.ZEBOV encoding the GP of the Ebola Zaire virus (Mayinga variant), followed by a second injection with multivalent MVA-BN-Filo encoding the GP of the Sudan and Zaire Ebola viruses and Marburg virus, together with Tai Forest virus nucleoprotein (Janssen Vaccines and Prevention B.V., the Netherlands and Bavarian Nordic, Denmark). Participants were randomly assigned into three Groups (1, 2, and 3) to receive one dose of Ad26.ZEBOV followed by MVA-BN-Filo on Day 29, 57, or 85, respectively. Whole blood samples collected into Tempus Blood RNA tubes (ThermoFisher Scientific) from 50 donors aged between 33 and 57 years, enrolled in France, were analyzed for this study ([Table 1](#)). Blood samples were taken at baseline of the Ad26.ZEBOV and MVA-BN-Filo injections and 3 h, 1 day, and 7 days later before storage at  $-80^{\circ}\text{C}$  ([Figure 1A](#)). The number of samples used in the transcriptome analysis in each time point were reported in the [Table 2](#).

**METHOD DETAILS**

**Assessment of ebola virus GP binding antibody concentrations**

Total IgG Ebola virus glycoprotein-specific binding antibody concentrations were measured by use of an Ebola virus glycoprotein Filovirus Animal Non-Clinical Group ELISA at Q2 Solutions Laboratories (San Juan Capistrano, CA, USA).<sup>16</sup>

**RNA extraction, library preparation, and sequencing**

Total RNA was purified from whole blood using the Tempus Spin RNA Isolation Kit (ThermoFisher Scientific). RNA was quantified using the Quant-iT RiboGreen RNA Assay Kit (Thermo Fisher Scientific) and quality control performed on a Bioanalyzer (Agilent). RNA samples were depleted of globin mRNA using the GlobinClear Kit (Invitrogen) prior to mRNA library preparation using NEBNext single cell/low input RNA library prep kit for Illumina (NEBNext Biolab). Libraries were sequenced on an Illumina HiSeq

2500 V4 system. Sequencing quality control was performed using Sequence Analysis Viewer (SAV). FASTQ files were generated on the Illumina BaseSpace Sequence Hub. Transcript reads were aligned to the hg18 human reference genome using Salmon v0.8.2<sup>102</sup> and quantified relative to annotation model “hsapiens-gene-ensembl” recovered from the R package biomaRt v2.42.1.<sup>101</sup> Quality control of the alignment was performed via MultiQC v1.4.<sup>102</sup> Finally, counts were normalized as log2 counts per million.

### Differential gene expression analysis

Differential gene expression analysis was performed with the *dearseq* package using mixed models with variance component test<sup>31</sup> to test the significance of differentially expressed genes at each post-injection time point of interest (3 h, 1 day, 7 days) compared to their respective baseline time points (1<sup>st</sup> or 2<sup>nd</sup> injection). The differentially expressed genes with adjusted p values (false discovery rate)  $\leq 0.05$  and fold-change in expression  $\geq \log_2 0.58$  (corresponding to a value of 1.5) were subjected to functional enrichment analysis using Ingenuity Pathway Analysis (IPA, Qiagen, <https://www.qiagenbioinformatics.com/products/ingenuity-pathway-analysis>) and Metascape<sup>112</sup> (<https://metascape.org>), and to pathway enrichment analysis using the cluster Profiler R package.<sup>104</sup> The tile plots were produced using the *ggplot2* R package.<sup>105</sup>

### Cell deconvolution analysis

The cell composition was inferred using the CIBERSORT algorithm,<sup>72</sup> implemented in the *tidybulk* package in R Bioconductor.<sup>106</sup> The proportion of immune cells is shown in a boxplot. Only cell populations that showed a significant difference between groups (Welch t test p value  $\leq 0.05$ ) are displayed.

### Construction of a protein–protein interactions (PPI) network

The interaction network among proteins encoded by candidate DEGs was established by importing genes into the STRING database v11.5 (<http://string-db.org>).<sup>107</sup> To remove PPI that were inconsistent from the dataset, we used the standard cut-off for the confidence interaction score  $\geq 0.4$ . Cytoscape<sup>108</sup> was used to construct the protein interaction association network and analyze the interaction association of the candidate DEGs. The node color represents the Z score of the mean of expression across patients for each time point.

### Molecular Complex Detection (MCODE) and identification

Cytoscape version 3.8.2 software was used for the gens network visualization. The MCODE plug-in<sup>109</sup> of the Cytoscape tool was used to visualize the significant gene modules in each network, with a cut-off k-core = 5 by default.

### Identification of DEGs correlating with antibody response after MVA-BN-FILO injection

For the determination of the DEGs that correlate with specific antibody production at 21 days post-MVA-BN-Filo and 364 days post-Ad26.ZEBOV vaccinations, we performed Lasso regression approach<sup>80</sup> using the 100 most modulated genes among the DEGs (FDR-adjusted p value  $\leq 0.05$ ; ranked by fold-change) at a given time point as the candidate correlates X variables with antibody levels (day 21 post-2<sup>nd</sup> injection and day 364 post-1<sup>st</sup> injection) as the response variable Y variables. The plots showing top ranked genes were produced using *glmnet* R package.<sup>113</sup> The Lasso coefficients provides information on a level of positive or negative association with the level of the EBOLA virus GP specific antibody response. The Lasso regression includes a regularization that shrinks insignificant variables completely to zero and removes them from the model. It thus results in a variable selection. We have also indicated the variation for each gene as expressed in log2 fold change, compared to before vaccination.

### Heatmap

ComplexHeatmap (v.2.2.0) was used for all heat maps.<sup>111</sup> All analysis were performed in the R (v.3.6.3) environment.

## QUANTIFICATION AND STATISTICAL ANALYSIS

Statistical analyses of differentially expressed genes at each post-injection time point of interest (3 h, 1 day, 7 days) compared to their respective baseline time points were performed with the *dearseq* package using mixed models with variance component test.<sup>31</sup> Differentially expressed genes with adjusted p values  $\leq 0.05$  and fold-change in expression  $\geq \log_2 0.58$  were considered statistically significant. The cell composition inferred using the CIBERSORT algorithm<sup>72</sup> was considered significantly different between groups when Welch t test p value  $\leq 0.05$ . The DEGs that correlate with specific antibody production at 21 days post-MVA-BN-Filo and 364 days post-Ad26.ZEBOV vaccinations, were determined with the Lasso regression approach<sup>80</sup> using the 100 most modulated genes among the DEGs (FDR-adjusted p value  $\leq 0.05$ ; ranked by fold-change) as the candidate correlates X variables with antibody levels as the response variable Y variables.